



1           **Environmental sequencing of marine protistan plankton communities**  
2   **reveals the effects of mesoscale cyclonic eddy transport on regional protistan**  
3   **diversity in subtropical offshore waters**

4

5

6

7           Sven Nicolai Katzenmeier<sup>1</sup>, Maren Nothof<sup>1</sup>, Hans-Werner Breiner<sup>1</sup>, Tim  
8   Fischer<sup>2</sup>, Thorsten Stoeck<sup>1</sup>

9

10

11

12   <sup>1</sup>Rheinland-Pfälzische Technische Universität Kaiserslautern-Landau, Ecology, D-  
13   67663 Kaiserslautern, Germany,

14   <sup>2</sup>GEOMAR Helmholtz Centre for Ocean Research Kiel, Germany

15

16

17

18

19   \*Corresponding author

20   Erwin-Schroedinger-Straße 14

21   D-67663 Kaiserslautern, Germany

22   email: [stoeck@rptu.de](mailto:stoeck@rptu.de)

23   phone: +49-631-2052502

24   fax: +49-631-205-2496

25



26           **Abstract**

27

28           Mesoscale eddies which origin in Eastern Boundary Upwelling Systems  
29 (EBUS) such as the Canary Current System entrap nutrient rich coastal water and  
30 travel offshore while ageing. We have analyzed the protistan plankton community  
31 structures in the deep chlorophyll maximum (DCM), sub-DCM and oxygen minimum  
32 zone (OMZ) of three differently aged cyclonic EBUS eddies off Northwest Africa as  
33 well as of non-eddy affected reference sites using DNA metabarcoding. Throughout  
34 all water depths, we found that the investigated eddies generated local dispersal-  
35 driven hotspots of protistan plankton diversity in the naturally oligotrophic subtropical  
36 offshore waters off Northwest Africa. Based on the taxonomic composition of protistan  
37 plankton communities, these diversity hotspots are likely to play an important role in  
38 carbon sequestration and for regional food webs up to top predatory levels. Thereby,  
39 the life-span of an eddy emerged as an important criterion, how local offshore protistan  
40 plankton diversity is transformed quantitatively and qualitatively: each of the three  
41 eddies was characterized by notably distinct protistan plankton communities. This  
42 could be linked to the physicochemical water properties (predominantly  
43 macronutrients, temperature and salinity) of the eddies' cores and rings, which  
44 experience pronounced changes during the eddies' westward trajectories.  
45 Furthermore, we found evidence that eddy-specific deep-water protistan communities  
46 are relatively short-lived compared to the ones in the sunlit DCM. However, our results  
47 do not only witness from the importance of fine-scale physical ocean features for  
48 regional ecosystem processes, but they also show the complexity of these ocean  
49 features and that we are still far from understanding the biological processes and their  
50 driving forces in such features.

51

52

53           *Keywords:* cyclonic eddies; diversity hotspots; DNA metabarcoding; eastern  
54 boundary upwelling system; mesoscale ocean features; oceanic carbon pump;  
55 protistan plankton

56

57

58

59



60           **1. Introduction**

61

62           Microbial eukaryotes (protists) play a vital role in the marine pelagic  
63 ecosystems. While marine phytoplankton account for only 1-2% of the total plant  
64 biomass globally, they contribute approximately 40% of the total fixed carbon on Earth  
65 (Falkowski, 1994). A key protistan plankton group is diatoms, which contribute ca. 40%  
66 of the primary production in the oceans (Falkowski et al., 1998). Bacterivorous  
67 protistan plankton (mostly heterotrophic nanoflagellates and small ciliates) are  
68 cropping bacterial production while herbivore protists (such as larger ciliates and  
69 heterotrophic dinoflagellates) routinely consume from 25% to 100% of the daily  
70 phytoplankton production, even in diatom-dominated upwelling blooms (Sherr and  
71 Sherr, 1994). Furthermore, protistan plankton channels carbon from lower trophic  
72 levels to multicellular organisms (Barber, 2007), explaining an aggregation of species  
73 of higher trophic levels in oceanic regions of high protistan plankton abundances. Not  
74 surprisingly, the diversity of protistan plankton strongly correlates with the diversity of  
75 consumers (García-Comas et al., 2016; Singer et al., 2021) making them key players  
76 in the success of fisheries (Chenillat et al., 2016). It has even been suggested that  
77 biogeographical diversity patterns estimated for primary producers may be used as a  
78 proxy of patterns for higher levels of the trophic chain (Duffy et al., 2007). Because of  
79 their high carbon transfer efficiency in the pelagic food web and their carbon export  
80 from the surface ocean to the deep-sea floor through sinking organisms, particles,  
81 aggregates or fecal pellets of primary consumers, oceanic protistan plankton is a  
82 pivotal component of the biological carbon pump. Because individual species of the  
83 protistan plankton have distinct carbon transfer or removal efficiencies (Degerman et  
84 al., 2018; Martin and Tortell, 2008; San Martin et al., 2006) the rate of carbon cycling  
85 and export from the ocean surface is heavily influenced by protistan plankton  
86 community composition (Brown et al., 2008; Legendre and Michaud, 1998; Michaels  
87 and Silver, 1988). Therefore, identifying patterns and hotspots of protistan plankton  
88 diversity in the global ocean is a cornerstone to improve our understanding of the local  
89 and global biological carbon pump.

90           Regions of highest protistan plankton productivity in the global ocean are areas  
91 with a high supply of nutrients, such as coastal upwelling regions (Pelegri et al., 2005;  
92 Van Oostende et al., 2018; Vargas et al., 2007; Ward et al., 2012). But also, the  
93 oligotrophic open ocean may experience oscillations in the nutrient regime, which



94 structure protistan plankton communities. As explained previously (Alexander et al.,  
95 2015) these oscillations may be driven by biological, anthropogenic or physical forcing.  
96 In the latter, meso- and sub-mesoscale physical processes such as eddies, fronts and  
97 filaments are of special importance as they are known to modulate the distribution and  
98 diversity of ambient plankton communities and their access to resources (Hernández-  
99 Hernández et al., 2020; Ramond et al., 2021).

100         The formation of eddies results mainly from baroclinic instability (Bibby et al.,  
101 2008; Kurian et al., 2011) due to e.g. the shearing from opposing currents, seafloor  
102 topology, upwelling filaments, wind forcing, coastline irregularities or a combination  
103 thereof (Batteen et al., 2003; McGillicuddy, 2016). In Eastern Boundary Upwelling  
104 Systems (EBUS) such as the Canary Current System (CanCS) off Northwest Africa,  
105 the formation of eddies is fueled by instabilities generated by velocity shear of the  
106 coastal current system and the Ekman circulation. In EBUS, eddies trap parcels of  
107 upwelled, nutrient-rich coastal water. Because the kinetic energy contained in the eddy  
108 field is often up to two orders of magnitude larger than the energy contained in the  
109 mean flow field (i.e. these eddies have a high rotational speed = high vorticity), the  
110 exchange between water masses trapped by the eddy and surrounding waters is  
111 severely limited (McGillicuddy, 2016). Thus, upwelled nutrients are advected offshore  
112 (up to several hundreds of kilometers) into the oligotrophic open ocean. Likewise,  
113 highly diverse plankton communities of upwelled coastal water become entrained into  
114 eddies and are transported offshore. These communities can undergo ecological  
115 succession as the eddies travel offshore and age (Brown et al., 2008; Cesar-Ribeiro  
116 et al., 2020; Owen, 1980).

117         Our knowledge on how protistan plankton diversity is associated with such  
118 meso- and sub-mesoscale processes is, however, scarce, mainly because such highly  
119 dynamic hydrographic features are difficult to locate and to sample (Ramond et al.,  
120 2021). While tidal fronts in coastal areas are recurrent and (relatively) easier to target  
121 for the study of in-situ protistan plankton diversity (Ramond et al., 2021), eddies  
122 provide a more challenging structure. Furthermore, the few previous studies that were  
123 dedicated to the investigation of protistan plankton diversity in eddies relied on  
124 microscopy-based identification of protistan plankton (Hernández-Hernández et al.,  
125 2020) or used chemotaxonomic methods such as CHEMTAX (Barlow et al., 2017;  
126 Carvalho et al., 2019). Even though these studies provided invaluable resources,  
127 chemotaxonomic methods have a low level of taxonomic resolution and may be



128 imprecise due the effects of nutrient availability on chlorophyll and other pigment ratios  
129 (Higgins et al., 2011). In microscopy-based diagnosis of protistan plankton community  
130 composition only a very limited number of plankton types was resolved (Abad et al.,  
131 2016; Eiler et al., 2013; Visco et al., 2015). Furthermore, classical taxonomic studies  
132 are extremely labor and time intensive and also expensive to acquire (Clayton et al.,  
133 2013). In addition, to the best of our knowledge, none of these previous studies that  
134 investigated protistan plankton community structure, appreciated the non-pigmented  
135 plankton types but focused exclusively on phytoplankton. The interrogation of  
136 taxonomic molecular barcodes obtained from environmental samples in combination  
137 with high-throughput sequencing and computational massive sequence data  
138 processing tools allows for in-depth insides into protistan plankton communities (Burki  
139 et al., 2021; Stoeck et al., 2010; Vargas et al., 2015). We here exploited this  
140 technology for the first study of protistan plankton diversity in three differently aged  
141 eddies originating in the Canary Current System off the Northwest African coast. In  
142 specific, we were asking how (quantitatively and qualitatively) cyclonic eddies affect  
143 the regional diversity of protistan plankton communities in a sub-tropical oligotrophic  
144 oceanic offshore region. Therefore, we analyzed samples from the deep-chlorophyll  
145 maximum (DCM), which holds a key role in ocean nutrient cycling, the biological  
146 carbon pump and the flow of energy (Cullen, 2015), from immediately below the DCM  
147 and from the oxygen minimum zone (OMZ), which is hypothesized to act as either a  
148 trap or as a sieve for the carbon export from eddies to the deep-sea (Chavez and  
149 Messié, 2009). Our results provide an unprecedented insight into the association of  
150 whole protistan plankton communities with ocean eddies in an eastern boundary  
151 region off Northwest Africa.

152

153

## 154 **2. Methods**

### 155 *2.1 Eddy descriptions and sample collections*

156 We sampled three differently aged cyclonic mesoscale eddies off the Northwest  
157 African coast during two cruises with RV *Meteor* (Fig. 1). Eddy “CE\_2019\_19N\_18W”  
158 (center coordinates: 18.73 N 18.03 W), which was closest to the coast, with an age of  
159 approximately two months, was sampled in June 2019 on cruise M156. Eddies  
160 “CE\_2019\_18N\_20W” (17.73 N 20.43 W) and “CE\_2019\_14N\_25W” (14.50 N 25.03  
161 W) were sampled on cruise M160 in December 2019. Eddy CE\_2019\_18N\_20W was



162 four months old, while CE\_2019\_14N\_25W was estimated to be six to seven months  
163 after formation while sampling. CE\_2019\_14N\_25W also changed from a typical eddy-  
164 like shape into an ellipsoid form at the ocean surface during the sampling process.  
165 The age of the eddies was determined using satellite data of surface level anomalies  
166 by Copernicus Marine Environment Monitoring Service (CMEMS;  
167 <http://marine.copernicus.eu>).

168 Sampling stations of the eddies were identified based on Archiving, Validation  
169 and Interpretation of Satellite Oceanographic data (AVISO) satellite images (Cesar-  
170 Ribeiro et al., 2020; Wu and Chiang, 2007). According to these satellite images  
171 sampling occurred along east-west and north-south transects through the eddy  
172 centers of CE\_2019\_18N\_20W and CE\_2019\_14N\_25W and an east-west transect  
173 only through eddy CE\_2019\_19N\_18W. For each transect, three sampling sites were  
174 chosen: one in the middle of the center, one approximately half way to the center  
175 periphery and one in the periphery (i.e., five sites for CE\_2019\_18N\_20W and  
176 CE\_2019\_14N\_25W; three sites for CE\_2019\_19N\_18W). The actual eddy  
177 dimensions and locations were later refined based on shipboard measurements.  
178 Based on these measurements, two sampling sites from CE\_2019\_18N\_20W and  
179 CE\_2019\_19N\_18W, each, and one sampling site from CE\_2019\_14N\_25W had to  
180 be excluded post hoc. These original sampling stations were actually outside of the  
181 eddy's zero-vorticity ring. At each sampling station (Table 1), we collected 20 L of  
182 water from the deep chlorophyll maximum (DCM), from right below the DCM and from  
183 the oxygen minimum zone (OMZ) using a Niskin Rosette equipped with a Seabird 911  
184 plus CTD system. The corresponding water depths are shown in Supplementary File  
185 2. Conductivity, temperature, oxygen and turbidity were obtained from the CTD. To  
186 accurately determine the dissolved oxygen concentration, volumetric titration was  
187 performed using the Winkler method (Strickland and Parsons, 1968; Wilhelm, 1888).  
188 Nutrient concentrations (phosphate ( $\text{PO}_4$ ), nitrate ( $\text{NO}_3$ ), orthosilicic acid ( $\text{Si}(\text{OH})_4$ )) of  
189 each layer were measured photometrically with an AutoAnalyzer (QuAAtro; Seal  
190 Analytical) using continuous flow analysis on unfiltered seawater for duplicate samples  
191 (Grasshoff et al., 2009).

192 To collect protistan plankton, water samples from Niskin bottles were drawn  
193 onto membrane filters (Durapore; Merck Millipore, Darmstadt, Germany; 0.65  $\mu\text{m}$  pore  
194 size, diameter 47 mm; ca. 3-5 liters per filter) using a peristaltic pump. Filters were  
195 then immediately transferred into a cryovial containing 3 ml nucleic acid preservation



196 solution (LifeGuard solution, Qiagen) and frozen at -20 °C until further processing in  
197 the laboratory. At each sampling site, three biological replicate filters were collected.

198

### 199 *2.2 Sample processing and high-throughput sequencing*

200 Total environmental DNA (eDNA) was extracted from each filter individually  
201 using Qiagen's DNeasy PowerWater kit according to the manufacturers protocol.  
202 From the extracted DNA we amplified the hypervariable V9 region of the small subunit  
203 ribosomal RNA (SSU rRNA) gene as a molecular taxonomic barcode following a  
204 standard protocol (Stoeck et al., 2010). The protocol employed 1391F as forward  
205 primer (5'-GTACACACCGCCCGTC-3'; (Lane, 1991)) and EukB as reverse primer (5'-  
206 TGATCCTTCTGCAGGTTACCTAC-3'; (Medlin et al., 1988)). The PCR protocol  
207 consisted of an initial denaturation step at 98°C for 30 s, followed by 30 cycles of 10 s  
208 at 98°C, 20 s at 61°C, 25 s at 72°C and a final five-minute extension at 72°C. The  
209 reactions volumes amounted to 50 µl and included 0.5 µl Phusion polymerase (New  
210 England Biolabs (NEB), Ipswich, MA, USA), 10 µl 5xPhusion GC buffer (NEB), 1 µl 10  
211 mM dNTPs, 0.5 µl template DNA, 32.5 µl PCR grade water, and 0.5 µl of each forward  
212 and reverse primer. Triplicate PCR reactions were run for each DNA extract to  
213 minimize PCR bias. Prior to purification (MinElute Kit; Qiagen), PCR sample replicates  
214 were pooled.

215 To prepare the resulting PCR products for high-throughput sequencing (HTS),  
216 sequencing libraries were constructed using the NEB Next Ultra DNA Library Prep Kit  
217 for Illumina (NEB). Library quality was assessed with an Agilent Bioanalyzer 2100  
218 system (Agilent, Santa Clara, CA, USA). Illumina MiSeq sequencing was conducted  
219 by SeqIT GmbH & Co. KG (Kaiserslautern, Germany). The sequence data files are  
220 deposited at the Sequence Read Archive of the National Center for Biotechnology  
221 Information under project number PRJNA795916.

222

### 223 *2.3 Sequence quality control, clustering and taxonomic assignment*

224 Illumina libraries were split based on the specific barcode identifiers of each  
225 individual sample and primers were removed from sequences using CUTADAPT  
226 v1.18 (Martin, 2011). Following, sequences were sorted in the same read direction  
227 with the FASTX toolkit (RRID: SCR\_005534). Sequences were then processed using  
228 the Divisive Amplicon Denoising Algorithm (DADA2, (Callahan et al., 2016)) using the  
229 DADA2 package v1.8 in R v4.0.5 as described for hypervariable taxonomic marker



230 genes from metabarcoding studies (Forster et al., 2019) with the model trained on  
231 Illumina runs and the following criteria: V9 SSU rRNA gene sequences were filtered  
232 using *filterAndTrim* with `truncLen=80` and `maxEE=1`. The truncation length criterion  
233 was determined by choosing the sequence position at which Phred assigned a quality  
234 score of  $\geq 30$  (Q3) for at least 51% of all reads in a dataset (=base call accuracy 99.9%,  
235 (Ewing and Green, 1998)). For `maxEE` we chose the most stringent value, to maximize  
236 the quality of the final sequence reads used for downstream analyses. Sequences  
237 from Read1 and Read2 were merged with the function *mergePairs* in DADA2 with a  
238 minimum overlap of 20 nucleotides and an allowed mismatch of 2. Potential chimeras  
239 were removed using the *uchime-denovo* algorithm (Edgar et al., 2011) in VSEARCH.  
240 Taxonomy was assigned with VSEARCH using the PR2 reference database for  
241 eukaryotic SSU rRNA gene sequences (Guillou et al., 2013), with the last common  
242 ancestor (LCA) as a decision criterion and a syntax cut-off of 0.8. To minimize  
243 ecologically uninformative noise, only ASVs with at least 2 reads were maintained for  
244 downstream analyses. The resulting ASV-to-sample matrix was then used for all  
245 statistical analyses. In the first step, we have analyzed the taxonomic composition on  
246 phylum level to identify the dominant phyla (in terms of assigned reads). For a higher  
247 taxonomic resolution, we then performed a more detailed analysis of these dominant  
248 phyla on family level. We refrained from increasing the taxonomic resolution beyond  
249 the family level because the proportion of unassignable ASVs on genus or species  
250 level was too high.

251

#### 252 *2.4 Statistical analyses*

253 Data analyses were conducted in R v. 4.0.5 using the program packages *vegan*  
254 (Oksanen et al., 2020) and *ggplot2* (Wickham, 2016) for graphical visualization.  
255 Similarity of sampling sites based on their physico-chemical properties was calculated  
256 and visualized by a principal component analysis (PCA) using the *rda* function.  
257 Physico-chemical parameters were scaled to a 0-1 value range using the *rescale*  
258 option of the *scale* package. Correlation of physico-chemical parameters with  
259 ordination axes were extracted from the PCA output.

260 Rarefaction analysis for each protistan plankton sample was conducted to  
261 assess the degree of sample saturation. Prior to the calculation of alpha- and beta-  
262 diversity measures, the number of sequences per sample was rarefied (normalized)





263 to the smallest sample size with the *rrarefy* function. In case of the complete dataset  
264 this was 131 108 sequences. We calculated the Shannon-Wiener Index  $H'$  and ASV  
265 richness as measures of alpha-diversity. The Bray-Curtis Index (BC) was used to  
266 calculate the similarity between samples based on the normalized ASV-to-sample  
267 matrix. BC similarity values were transformed to a distance matrix for a non-metric  
268 multidimensional scaling (NMDS) analysis using the *metaMDS* function with default  
269 settings. Vectors were fitted to the ordination using the *envfit* function of the *vegan*  
270 package in R. The fit ( $R^2$ ) of each variable to the ordination using the *envfit* function  
271 was assessed with a Monte Carlo analysis of 1,000 permutations. In addition to a beta-  
272 diversity analysis of all samples, we conducted a beta-diversity analyses for each  
273 individual sampling depth (DCM, below DCM and OZM). Therefore, we normalized  
274 each of the three datasets to the smallest sample size within these datasets (214,045  
275 for the DCM dataset, 131,108 for the below DCM dataset and 237,637 for the OMZ  
276 dataset). This allowed to exploit the maximal information included in each individual  
277 dataset. BC similarity for the individual depth layers was then visualized in distance  
278 dendrograms.

279

### 280 **3. Results**

#### 281 *3.1 Physicochemical structures of the eddy and reference samples*

282 Vertical CTD profiles of physico-chemical data as well as nutrients at the  
283 sampling sites (eddies and reference stations) are provided as Supplementary Files 1  
284 and 2. Here, we focus on the most prominent physico-chemical differences between  
285 the three eddies CE\_2019\_19N\_18W, CE\_2019\_18N\_20W and CE\_2019\_14N\_25W  
286 and the two reference sites. In a principal component analysis (PCA) based on the  
287 physico-chemical data, the three depth layers (DCM, sub-DCM, OMZ) followed a  
288 gradient along PCA axis 1, while the three eddies had a notably stronger association  
289 with an axis-2 gradient (Fig. 2). Axis 1 explained as much as 93.2% of the observed  
290 variation. As a rule, concentrations of macronutrients and silicate increased from DCM  
291 to sub-DCM and OMZ, while salinity, fluorescence, temperature and dissolved oxygen  
292 decreased. Differences in physicochemical parameters were notably more  
293 pronounced in the DCM samples. The sub-DCM and the OMZ, were increasingly more  
294 similar in their physicochemical properties. In the OMZ, even the reference samples  
295 clustered with the eddy samples. We were not able to identify the physico-chemical  
296 parameters that separated the samples within each depth layer and eddy along PCA



297 axis 2. It is noteworthy, that among all DCM samples, the youngest eddy  
298 CE\_2019\_19N\_18W which was still closest to the coast was characterized by the  
299 lowest concentrations of macronutrients and silicate. Furthermore, temperature and  
300 salinity were notably lower compared to the other DCM samples.

301

### 302 *3.2 Sequence data overview*

303 After cleaning of the obtained raw sequence datasets, we retained between  
304 131 108 (min) and 1 2619 83 (max) high quality (HQ) sequences (SI Table 3).  
305 Subsequently, normalization of read counts to the minimum sequence number was  
306 applied for the complete dataset and also for each depth layer separately to account  
307 for differences in sequencing depth. This resulted in 131 108 (complete data set), 214  
308 045 (DCM), 131 108 (sub-DCM) and 237 637 (OMZ) reads per sample. Rarefaction  
309 profiles showed that all samples were sequenced to near saturation (SI Fig. 4).

310

### 311 *3.3 Alpha diversity of protistan plankton communities*

312 The normalized ASV richness as well as the Shannon Index  $H'$  as measures of  
313 alpha diversity were largely congruent for all samples (Fig. 3). Eddy  
314 CE\_2019\_18N\_20W had a significantly lower  $H'$  compared to the oldest  
315 CE\_2019\_14N\_25W eddy across all samples  $p < 0.05$ ). The same eddy had  
316 significantly lower ASV richness and  $H'$  compared to the background reference waters  
317 of CB and CVOO (across all depth, Bonferroni corrected  $p < 0.005$  in both cases).  
318 Thus, eddy CE\_2019\_18N\_20W stood out as the eddy with the lowest overall alpha  
319 diversity. We did not find significant differences in ASV richness and  $H'$  when  
320 comparing DCM, sub-DCM and OMZ with each other. In more detail, the overall  
321 highest ASV richness was obtained for a sample from the sub-DCM of the six to seven  
322 months old CE\_2019\_14N\_25W eddy (sample 1: 4454 ASVs) and the lowest for an  
323 OMZ sample from eddy CE\_2019\_18N\_20W (4: 1037). The overall highest  $H'$  was  
324 obtained for an OMZ sample of eddy CE\_2019\_14N\_25W (3: 6.53) and the lowest for  
325 an OMZ sample of eddy CE\_2019\_18N\_20W (4: 3.27). In the DCM (Fig. 3a), none of  
326 the eddy protistan plankton communities was as diverse ( $H'$ ) and ASV-rich as any of  
327 the two background reference waters. This was in sharp contrast to the OMZ (Fig. 3c),  
328 in which plankton communities of the CE\_2019\_14N\_25W eddy were notably more  
329 diverse compared to the ones of the two other eddies and also to both reference sites  
330 (except  $H'$  for sample CE\_2019\_14N\_25W(1) compared to CVOO reference).



331 Plankton communities of eddy CE\_2019\_18N\_20W were the least diverse in the OMZ.  
332 In the sub-DCM (Fig. 3b) lowest ASV richness was measured in the youngest eddy  
333 CE\_2019\_19N\_18W and lowest  $H'$  in eddy CE\_2019\_14N\_25W.

334 In the second step, we analyzed to what extent the three different eddies  
335 increased the regional protistan plankton diversity of the background waters  
336 (reference samples) (Fig. 4) by the eddy-induced transport of eddy-specific protistan  
337 communities into offshore regions under study. In terms of ASV richness (Fig. 4a), all  
338 eddies increased the regional diversity notably. The six to seven months old eddy  
339 CE\_2019\_14N\_25W increased regional diversity the most (220 % integrated over all  
340 depth for CB background waters and 171% for CVOO background waters). The least  
341 impact on protistan ASV richness was obtained for the youngest eddy  
342 CE\_2019\_18N\_20W (178 % integrated over all depth for CB background waters and  
343 146% for CVOO background waters). Interestingly, the increase of regional ASV  
344 richness was typically higher in deeper waters (sub-DCM and OMZ) compared to the  
345 sunlit DCM. The Shannon diversity  $H'$  did not mirror the ASV richness pattern (Fig.  
346 4b). As a rule,  $H'$  increased only marginally due to the introduction of a new community  
347 into the CB and CVOO background waters, or even decreased slightly, especially in  
348 case of the four-months aged eddy CE\_2019\_18N\_20W in all depths.

349

### 350 *3.4 Beta diversity*

351 In a nonmetric multidimensional scaling (NMDS) of Bray Curtis (BC) distances  
352 of all samples, protistan plankton communities showed a clear pattern (NMDS stress:  
353 0.121, Fig. 5). Samples from the different depth layers DCM, sub-DCM and OMZ  
354 (including the reference samples) were distributed predominantly along NMDS axis 1,  
355 with a gradient from the DCM towards the OMZ from lower to higher axis 1 values.  
356 Samples from the individual eddies were largely following a gradient along axis 2, with  
357 samples from the youngest eddy CE\_2019\_19N\_18W in the lower axis 2 value range.  
358 Protistan communities from the oldest CE\_2019\_14N\_25W eddy appeared as an  
359 intermediate between the young CE\_2019\_19N\_18W eddy and the four-month-old  
360 CE\_2019\_18N\_20W eddy. Within the individual depth layers, the protistan plankton  
361 communities of the two reference sites were as dissimilar to each other as were the  
362 protistan plankton communities of two different eddies. It is noteworthy that in the  
363 OMZ, the protistan plankton community structure of one individual sample from the  
364 eddy CE\_2019\_14N\_25W (1) was remarkably different from the two other OMZ



365 samples of this eddy. Several environmental parameters were strongly correlated with  
366 the NMDS axes with significant p-values (Table 2). The gradient along axis 1 from the  
367 shallower DCM towards the deeper OMZ was positively correlated with nutrients  
368 (nitrate, phosphate, orthosilicic acid, all of which had a high correlation coefficient),  
369 and negatively with temperature, salinity, oxygen (low correlation coefficient) and  
370 density, all of which were functions of the water depth. *Chla*-fluorescence and turbidity  
371 (low correlation coefficient) were also negatively correlated with the gradient from the  
372 DCM towards the OMZ. None of the tested environmental parameters were  
373 particularly strongly correlated with NMDS axis 2. Therefore, the parameters  
374 structuring protistan plankton communities of the individual eddies within each of the  
375 three depth layers remained largely obscured.

376 For a more detailed comparison of protistan plankton communities within each  
377 of the three depth layers individually, we constructed BC-based dendrograms for the  
378 DCM (Fig. 6a), the sub-DCM (Fig. 6b) and the OMZ (Fig. 6c). These analyses made  
379 obvious that the structuring of protistan plankton communities followed different  
380 patterns in the three depth layers. In the DCM, protistan plankton communities trapped  
381 in all three eddies as well as the ones of the two reference stations formed individual  
382 clusters. Thereby, the DCM protistan plankton community of the youngest eddy  
383 CE\_2019\_19N\_18W was most similar to the ones of the two reference sites. In the  
384 next deeper water layer, the sub-DCM, both reference sites fell into the same cluster  
385 as the samples from the CE\_2019\_14N\_25W eddy, indicating the relatively high  
386 similarity of the protistan plankton communities in the deeper water layers of the  
387 CE\_2019\_14N\_25W eddy to the non-eddy-disturbed open ocean. Protistan plankton  
388 communities trapped in eddy CE\_2019\_19N\_18W and the aged eddy  
389 CE\_2019\_18N\_20W each remained as separate clusters. In the deepest water layer,  
390 the OMZ, only the protistan plankton communities trapped in the aged eddy  
391 CE\_2019\_18N\_20W formed an eddy-specific cluster, while all other samples merged  
392 in the same cluster. This indicates that in the young CE\_2019\_19N\_18W and the  
393 oldest CE\_2019\_14N\_25W eddy, the protistan plankton community structures were  
394 relatively similar to the ones in the non-eddy-disturbed open ocean.

395

### 396 *3.5 Taxonomic composition of protistan plankton communities*

397 In the DCM of all samples (SI Fig 5 a), sequences assigned to dinoflagellates  
398 had the highest relative abundance. As a rule, these were followed by radiolarians,



399 Discoba and haptophytes. Anomalies on phylum-level taxonomy in the DCM worth  
400 emphasizing were that the youngest eddy CE\_2019\_19N\_18W stood out for its higher  
401 proportion of chlorophyte-assigned sequences and lower proportion of sequences  
402 assigned to Discoba compared to all other samples. Likewise, sub-DCM and OMZ  
403 samples were dominated by sequences assigned to dinoflagellates, radiolarians,  
404 Discoba and haptophytes (SI Fig 5 a). In the following we describe the taxonomic  
405 inventory of these four most abundant taxon groups in a higher taxonomic resolution.  
406 Because the variation of the taxonomic assignments of sequence reads was typically  
407 notably smaller among samples of the same eddy and depth compared to the inter-  
408 sample comparison we averaged the taxonomic assignments for the following sub-  
409 groups per eddy and depth layer, which facilitates the diagnosis of differences and  
410 similarities among eddies, different water depth layers and the reference background  
411 waters.

412 *Haptophyta* (SI Fig 5 b). In the DCM, haptophytes were dominated in all  
413 samples by Chrysochromulinaceae and Phaeocystaceae. In the youngest eddy  
414 CE\_2019\_19N\_18W, the relative read abundance of Chrysochromulinaceae was  
415 notably higher compared to all other samples, accounting for nearly 90% of all  
416 haptophyte-assigned sequence reads. Phaeocystaceae were accordingly less  
417 abundant in the DCM core of CE\_2019\_19N\_18W compared to all other samples.  
418 This also applied to unassigned Prymnesiophyceae, which accounted for roughly a  
419 quarter of the sequence reads in both background waters (reference samples) and for  
420 10% and 20% in eddies CE\_2019\_18N\_20W and CE\_2019\_14N\_25W, respectively.  
421 Furthermore, it is noteworthy that HAP-clade II sequences were negligible in all eddy  
422 DCM samples, but accounted for 5% and 14% in references Cape Blanc and CVOO.  
423 In the deeper sub-DCM waters, the proportion of the HAP-clade 4 increased  
424 remarkably, particularly in the two background waters Cape Blanc and CVOO and the  
425 cone shaped eddy CE\_2019\_14N\_25W, but also, to a notably lesser extent, in the  
426 other sub-DCM samples. In the young eddy CE\_2019\_19N\_18W, HAP-5 clade  
427 assigned sequences accounted for the majority (43%) of haptophyte sequences at the  
428 cost of Chrysochromulinaceae, which declined vastly from DCM to sub-DCM. In the  
429 sub-DCM of the four-months aged eddy CE\_2019\_18N\_20W, Phaeocystaceae were  
430 dominating and accounted for 81% of all haptophyte sequence reads.

431 *Radiolaria* (SI Fig 5 c). Spumellarida (unassigned and Spumellarida Group I)  
432 belonged to the most abundant radiolarians in terms of relative sequence reads with



433 a remarkable increase of Spumellarida Group I from the DCM to the sub-DCM and the  
434 OMZ in all samples. In the DCM, the young eddy CE\_2019\_19N\_18W had by far the  
435 highest proportion of Arthracanthida-Symphycanthida- and Collospheridae-assigned  
436 sequences, accounting together for 63% of all radiolarian sequences in the DCM of  
437 CE\_2019\_19N\_18W. The aged eddy CE\_2019\_18N\_20W stood out from the other  
438 samples because of its relatively high proportions of acantharean and RAD-B group 1  
439 sequence reads in the DCM. The DCM of the oldest eddy CE\_2019\_14N\_25W as well  
440 as the CVOO background waters had relatively high proportions of Polycystinea  
441 (including Collodaria and Nasselaria) compared to all other samples (21% and 16%  
442 respectively).

443 *Discoba* (SI Fig 5 d). The vast majority of *Discoba*-assigned sequence reads in  
444 all samples (up to 98%, Cape Blanc OMZ reference) belonged to unidentified  
445 *Diplonema* that could not be further classified. The DCM-and sub-DCM samples of the  
446 young eddy CE\_2019\_19N\_18W as well as the deep-water OMZ samples of the eddy  
447 CE\_2019\_14N\_25W stood out from the other samples by their relatively high  
448 proportions of DSPD-1 (deep-sea pelagic diplonemids group 1).

449 *Dinoflagellata* (SI Fig 5 a). The composition of the dinoflagellate communities is  
450 relatively consistent across all eddies, the background waters and also across all  
451 vertical water layers. The vast majority of sequence reads in all samples belong to the  
452 two taxonomic clades Dino-Group I and Dino-Group II (also termed Marine Alveolates  
453 Group I and II or Syndiniales Group I and II). The youngest eddy CE\_2019\_19N\_18W  
454 stands out from all other samples because of its relatively high proportion of Dino-  
455 Group III sequence reads, particularly in the sub-DCM. The high proportion of  
456 unassigned Dinophyceaea, which included numerous ecologically distinct orders,  
457 decreased remarkably from DCM to sub-DCM and OMZ. Similarly remarkable is the  
458 high proportion of unassigned dinoflagellates which increased from DCM to sub-DCM  
459 and OMZ in all samples. In sum, both groups of sequence reads that escaped further  
460 taxonomic classification accounted for up to 43% (DCM of Cape Blanc background  
461 water) of all dinoflagellate-assigned sequence reads in the oceanic region under  
462 study.

463

464 Supplementary File 6 provides a higher-resolution taxonomy assignment for all  
465 samples (ASV-to-sample matrix).

466



467

468

469

## 4. Discussion

470

471

472

### 4.1 Effect of eddies on regional protistan plankton diversity

473

474 A previous field survey demonstrated that the diversity of protistan plankton in  
475 ocean surface waters (including the DCM) follows a pronounced, mainly temperature-  
476 driven, latitudinal diversity gradient with an increasing Shannon diversity from polar  
477 regions to the equatorial tropics (Ibarbalz et al., 2019). This agrees well with an in  
478 silico obtained global pattern for marine phytoplankton (Barton et al., 2010). Thus,  
479 both studies identify the subtropical, low-seasonality oceanic region as locations of  
480 moderate protistan plankton diversity. This agrees well with the findings of this study  
481 (see Shannon diversity and ASV richness of reference samples, Fig. 3). Our results  
482 showed that dispersal through eddies enhanced this moderate regional diversity of  
483 protistan plankton communities in a subtropical oceanic offshore region. When  
484 combining protistan communities from reference samples with the protistan  
485 communities introduced to the oligotrophic offshore regions, the regional diversity  
486 even increases the global diversity peaks of whole protistan plankton communities in  
487 tropical oceanic regions (Ibarbalz et al., 2019).

487

488 This finding is consistent with predictions from ecological theory, which  
489 considers the role of dispersal in relation to diversity patterns: with increasing rates of  
490 dispersal, the corresponding model predicts an increase in alpha-diversity, while  
491 regional beta-diversity decreases (Cadotte, 2006). Global numerical simulations  
492 investigating the effects of eddies on marine phytoplankton diversity predicted that  
493 eastern boundary regions such as the one under study are dispersal driven hotspots  
494 of diversity. This is in contrast to western boundary regions such as the Agulhas  
495 system, which is a locally driven plankton diversity hotspot (Clayton et al., 2013).  
496 These numerical simulations by Clayton and colleagues (2013) provided modelled  
497 predictions of patterns in diversity and hypotheses regarding the mechanisms that  
498 control them, which prior to our study has gone untested for whole protistan plankton  
499 communities in eastern boundary regions. Our field study provides support for these  
500 simulated predictions for eastern boundary regions.

500

501

In general, the richness of plankton communities at any location is a composite  
of the richness of immigrant plankton types ( $a_i$ ) plus the richness of locally adapted



502 types ( $a_{ia}$ ). Locally adapted types thrive in the local environment with a net population  
503 growth, which is balanced by export through advection or mixing processes.  
504 Conversely, immigrant types are maintained by a source due to transport from  
505 elsewhere, such as eddies. They are not ideally adapted to local environmental  
506 conditions. Loss due to competitive exclusion balances the source, and immigrant  
507 types would disappear from the local populations if transport were shut off (Clayton et  
508 al., 2013; Ward et al., 2021). Because the regional protistan plankton diversity in the  
509 subtropical offshore regions under study was driven by the transport and convergence  
510 of plankton types from different regions, we can clearly confirm model predictions  
511 which suggest that eastern boundary regions are dispersal-driven plankton diversity  
512 hotspots rather than locally driven hotspots. This corroborates with the hypothesis that  
513  $a_i$  is quantitatively of higher importance ( $a_i > a_{ia}$ ) for the regional diversity in sub-tropical  
514 and tropical regions compared to temperate and polar regions (Clayton et al., 2013).  
515 In contrast, the four western boundary regions are confluences of different water  
516 masses, each bringing their resident phytoplankton populations (d'Ovidio et al., 2010).  
517 One would therefore expect a similar immigration-driven diversity hotspot scenario in  
518 western boundary regions compared to the sub-tropical eastern boundary regions.  
519 However, most of these immigrants are able to thrive in the confluence regions,  
520 because the local growth of the immigrants after shutoff from transport is supported  
521 by an enhanced supply of nutrients associated with the typical confluence of western  
522 boundary systems. Therefore, eddy-fueled dispersal effects on regional protistan  
523 diversity in western boundary systems, such as differently aged Agulhas rings (Cesar-  
524 Ribeiro et al., 2020) is substantially different from the one in eastern boundary regions  
525 (this study).

526         The increase of regional protistan ASV richness through eddy dispersal  
527 occurred in all three water layers sampled (DCM, sub-DCM and OMZ). An at first sight  
528 peculiar finding was that the relative change in the Shannon diversity index  $H'$  was to  
529 a much lesser extent affected by immigration than the regional ASV richness.  
530 Furthermore, differences became evident in a direct comparison between these two  
531 quantities. Such observations, however, are not unusual and can be explained as  
532 follows:  $H'$  (Shannon and Weaver 1949) is a measure of both, the protistan plankton  
533 ASV richness and the evenness of the protistan plankton communities. This is an  
534 index of species diversity and not of species richness. The latter is just one component





535 of species diversity and refers to the number of species. A detailed discussion on this  
536 subject was published previously by (Spellerberg and Fedor, 2003). An increase in  
537 regional protistan plankton richness introduced by immigrants of the aged eddy  
538 CE\_2019\_18N\_20W is therefore not in contradiction to a decreased  $H'$  relative to both  
539 reference samples, but highlights a community with a high species (ASV) richness and  
540 a low evenness, i.e., few ASV are highly dominant in their sequence read abundance,  
541 outnumbering the vast majority of other less-abundant species in the protistan  
542 community. This is most likely an effect of the evolution of protistan communities in  
543 ageing eddies.

544

#### 545 **4.2 Species (ASV) richness, diversity and taxonomic composition of** 546 **protistan plankton communities in eddies propagating from the Northwest** 547 **African coast**

548 All three eddies investigated in this study are different in their ASV richness,  
549 diversity and taxonomic composition, and thus, affected regional protistan plankton  
550 diversity qualitatively and quantitatively in different ways. We here discuss the  
551 differences in protistan plankton community structures among the three differently  
552 aged eddies to assess their individual effects on regional offshore waters along their  
553 trajectories. We, however, refrain from discussing our results in the context of  
554 succession patterns of ageing eddies. Such a study would require the sampling of the  
555 same eddy on a high temporal and also spatial scale.

556 We found the most pronounced differences in protistan plankton communities  
557 among the three eddies under study in the DCM, while in sub-DCM and the OMZ the  
558 communities become increasingly more similar, which corroborated with the  
559 physicochemical profiles of the eddies. The DCM of the youngest eddy  
560 CE\_2019\_19N\_18W, sampled closest to the Mauritanian coast, had the least diverse  
561 protistan plankton community and lowest ASV richness, enhancing the plankton  
562 diversity of the regional offshore background water to a lesser extent than eddies  
563 CE\_2019\_18N\_20W and CE\_2019\_14N\_25W. Its physicochemical properties with  
564 relatively low temperature, salinity and chlorophyll fluorescence in the DCM are typical  
565 properties of a younger cold core eddy. Warmer higher-salinity surface water masses  
566 form a ring-like structure around colder upwelled nutrient-rich water that is feeding the  
567 Canary Current System. This forms a structure consisting of the center of the eddy  
568 (cold core), an outer swirling ring, and the surrounding background water



569 (Dilmahamad et al., 2021). Such eddies typically contain a variety of waters with  
570 differing temperature-salinity characteristics, and the fine-scale variability is especially  
571 high in the core of the eddy (Leach and Strass, 2019). Due to a strong stratification  
572 between these water masses, the core usually maintains its distinctive  
573 physicochemical properties after propagation from the coast and during its trajectory  
574 towards offshore regions. Even though leakage or intrusion of background water is not  
575 unusual, depending on changes in velocities across the vertical eddy profile, seasonal  
576 and hydrographic effects, split, merge and linking events, eddy core and ring  
577 structures, and eddy shapes (Hall and Lutjeharms, 2011; Lamont and Barlow, 2017;  
578 Liu et al., 2019). This may further influence not only physicochemical properties but  
579 also protistan plankton communities in the eddy core.

580 We found some evident taxonomic signatures that distinguished the DCM of  
581 eddy CE\_2019\_19N\_18W from the offshore reference sites and also from the other  
582 two eddies. These signatures strongly indicate the confluence of (near-coastal) sunlit  
583 surface waters and upwelled deep-water masses. Such a relatively high abundance  
584 of Chlorophyceae as we detected in the DCM of eddy CE\_2019\_19N\_18W is atypical  
585 for offshore as well as for deep waters from the non-photic zone. This class of green  
586 algae prefers colder and low salinity waters, such as we found in the DCM core of  
587 CE\_2019\_19N\_18W, as well as sunlit surface and coastal waters (Tragin and Vaultot,  
588 2018). Likewise, the relative to other samples higher abundance of sequence reads  
589 assigned the radiolarian Arthracanthida-Symphyacanthida clades in the DCM of  
590 CE\_2019\_19N\_18W witnesses from a seed community in the eddy core that is  
591 partially recruited from surface waters. This taxon group is photosymbiotic and  
592 possesses robust skeletons withstanding turbulent waters (Decelle et al., 2012).  
593 Arthracanthida and Symphyacanthida complete their full life cycles in the photic zone  
594 because they are not capable of forming cysts and each new generation is forced to  
595 recruit new phototrophic endobionts (Decelle et al., 2013; Martin et al., 2010). Thus,  
596 their abundances typically decrease with water depth (Mars Brisbin et al., 2020). The  
597 notably lower abundances of Arthracanthida and Symphyacanthida in the DCM of  
598 other samples analyzed in this study may point to the low competitiveness of these  
599 taxon groups when nutrients and micronutrients (such as strontium needed for the  
600 skeleton) become depleted. Another noteworthy signature is the high read abundance  
601 of the haptophyte *Chrysochromulina* in CE\_2019\_19N\_18W compared to all other DCM  
602 samples. *Chrysochromulina* is a globally distributed marine pico- to nano-sized



603 phototrophic flagellate (Estep and MacIntyre 1989). Some species are also capable  
604 of phagotrophy and the balance between phagotrophy and photosynthesis seems to  
605 be influenced by environmental factors (Flynn and Mitra, 2009; Wilken et al., 2020).  
606 Favorable conditions to trigger growth of *Chrysochromulina* include a combination of  
607 lower salinities, higher macronutrient concentrations, also higher concentrations of  
608 nitrogen compounds and higher N:P ratios (Dahl et al., 2005), all of which are the case  
609 for the DCM core waters of CE\_2019\_19N\_18W compared to the other eddies and  
610 the reference stations. *Chrysochromulina* species can form massive blooms and  
611 produce hypertoxins as a metabolic response to cellular stress triggered by  
612 environmental and physiological factors, presumably to outcompete other  
613 phytoplankton (Johansson and Granéli, 1999). Such toxins can cause massive fish  
614 kills and severe economic damage (Anderson et al., 2000). On the other hand,  
615 *Chrysochromulina* species are major players for the ocean carbon cycle and carbon  
616 sequestration (Fixen et al., 2016; Hovde et al., 2015), but also contribute to methane  
617 oversaturation in marine waters, and, thus, are important organisms when studying  
618 climate-relevant processes in marine surface waters (Klitzsch et al., 2019). To the  
619 best of our knowledge, *Chrysochromulina* blooms have thus far not yet been reported  
620 from marine waters off West Africa (Hallegraeff et al., 2021). The higher proportion of  
621 the *Discoba* group DSPD-1 (deep-sea pelagic diplomonads) in the DCM of  
622 CE\_2019\_19N\_18W is biological evidence for the entrapping of relatively recent  
623 upwelled nutrient rich water from deeper water layers. This remarkably diverse group  
624 of heterotrophic excavate flagellates from mesopelagic layers has come to attention  
625 relatively recently through massive environmental sequencing surveys (Lara et al.,  
626 2009; López-García et al., 2001; Scheckenbach et al., 2010). Reports from the photic  
627 zone are rare (Flegontova et al., 2016) and the formation of eddies in upwelling regions  
628 provides an hitherto undescribed mechanisms to transport these typical dark ocean  
629 inhabitants to the sunlit surface layers. Flegontova et al. (2016) emphasized in their  
630 detailed study about diplomonads that “So far, no DSPD I diplomonad has been formally  
631 described, and we know nothing about their biology.” The observation that other DCM  
632 samples have much lower proportions of DSPD indicates that DSPDs are no  
633 successful competitors while residing in the DCM as the eddies age and travel further  
634 offshore. The extremely high proportion of unassigned diplomonads in all DCM  
635 samples shows that we are still far from knowing and understanding the diversity and  
636 ecology of these enigmatic organisms. The offshore waters of the Northwestern



637 African coast are a new valuable source for further diplonemid-focused studies.  
638 Diplonemid communities are stratified according to depth (Flegontova et al., 2016).  
639 Given the high proportion of these new diplonemid sequences in all DCM samples it  
640 is reasonable to assume that the corresponding organisms may belong to the photic  
641 zone diplonemid community (Flegontova et al., 2016; Vargas et al., 2015) and have  
642 corresponding metabolic and competitive properties. This, however, remains to be  
643 validated in further studies of diplonemids in this oceanic offshore region.

644 In contrast, macronutrients in the DCM of the four-months aged eddy  
645 CE\_2019\_18N\_20W were largely depleted, selecting for taxa better adapted to low-  
646 nutrient conditions. The haptophyte algae Phaeocystaceae is most abundant in the  
647 nutrient-depleted DCM of eddy CE\_2019\_18N\_20W. *Phaeocystis* is the only  
648 described genus in this family (Adl et al., 2019), and, like other haptophytes, plays a  
649 key role in ocean carbon cycling (Smith et al., 1991), but also in the sulfur cycle  
650 because of its significant dimethyl sulfide (DMS) production (Liss et al., 1994).  
651 *Phaeocystis* species evolve in nutrient, especially nitrogen rich waters (Schoemann et  
652 al., 2005; Smith et al., 1991), as can be found in freshly upwelled and trapped nutrient  
653 rich water in younger eddies such as CE\_2019\_19N\_18W. This alga is a major  
654 consumer of nitrogen, and may have contributed significantly to the nitrogen depletion  
655 in the DCM of eddy CE\_2019\_18N\_20W, while fixing inorganic carbon. A very similar  
656 scenario was described for *Phaeocystis* in polar waters that started to bloom at high  
657 nitrogen concentrations and then consumed the nitrogen in the water to depletion  
658 (Smith et al., 1991). However, *Phaeocystis* species are also among the dominant  
659 endosymbionts of actinophorean Radiolaria in warm oligotrophic oceanic regions  
660 (Decelle et al., 2012; Mars Brisbin et al., 2018). The symbiosis between *Phaeocystis*  
661 and acanthareans is an ecologically relevant mechanism to enable primary production  
662 hotspots in low-nutrient regions (Decelle et al., 2013). This corroborates well with our  
663 finding that the relative proportion of (unidentified) acanthareans is also highest in the  
664 eddy CE\_2019\_18N\_20W DCM samples compared to all other DCM samples.  
665 Acanthareans belong to the microplankton and have a mixotrophic lifestyle as an  
666 adaptation to low-nutrient conditions. They provide their algal symbionts with nutrients,  
667 which they acquire through predation. In return, the phototrophic symbiont provides  
668 carbohydrates produced during photosynthesis. The energy that acanthareans gain  
669 from these carbohydrates does not only make them strong competitors in nutrient  
670 depleted environments such as in the core of eddy CE\_2019\_18N\_20W, but also



671 provides additional energy which is required to maintain the strontium sulfate  
672 skeletons of acanthareans (Decelle et al., 2013, 2012). Furthermore, the DCM core of  
673 eddy CE\_2019\_18N\_20W had higher proportions of the dino-group II, a taxonomic  
674 group consisting of diverse Syndiniales phylotypes with *Amoebophrya* being the only  
675 described genus. Syndiales group II (also called marine Alveolates Group II (MALV II,  
676 (Groisillier et al., 2006)) is one of the dinoflagellate groups that is responsible for the  
677 overwhelming numerical dominance of dinoflagellate sequences in all samples  
678 analyzed in this study, the other one being MALV I. All Syndiniales have a parasitic  
679 lifestyle are parasitoids and obligately kill their hosts. Hosts of Group II include  
680 predominantly other dinoflagellates and also acanthareans, as well as other  
681 radiolarians and Cercozoa (Guillou et al., 2008; Siano et al., 2011). Thus, Group II  
682 phylotypes may play an important role in the top-down control of plankton  
683 communities. Survival of the dinospores in the water after release from the killed host  
684 lasts only for few days (Coats and Park, 2002). Therefore, it is reasonable to assume  
685 that at least most of the recorded sequence reads come from actual host infections.  
686 Most sequences obtained from environmental studies that were assigned to Group II  
687 originated from waters of the oxygenated photic zone (Guillou et al., 2008). In the  
688 winter months, Syndiniales Group II phylotypes were so abundant in oligotrophic DCM  
689 offshore waters of South Benguela that they were the most dominant taxon group in  
690 the plankton (Rocke et al., 2020). But also in other oceanic regions, MALV II  
691 phylotypes belong numerically to the most dominant sequences in protistan plankton  
692 metabarcoding datasets (Vargas et al., 2015). MALV I ASVs were in contrast  
693 predominantly (but not exclusively) retrieved from low-oxygen or anoxic marine waters  
694 (Guillou et al., 2008). Based on the results obtained in this study, we find no support  
695 of the hypothesis that MALV I ASVs prefer oxygen-depleted environments. Our study  
696 is the first one to report such a dominance of dinoflagellates from the oceanic region  
697 under study. A remarkably high proportion of the detected dinoflagellate communities  
698 in this oceanic region seems morphologically unknown as we conclude from the high  
699 proportion of taxonomically unassigned dinoflagellate sequences. Furthermore,  
700 MALVs, which account for the vast majority of detected dinoflagellate sequences in  
701 our study, usually escape light microscopy diagnosis. To better understand the  
702 ecological role of these abundant organisms in the DCM core of eddy  
703 CE\_2019\_18N\_20W and in the oceanic region under study, future research should  
704 focus on the identification of host-parasite relationships and their spatio-temporal



705 patterns. But also more detailed morphological inventories of protistan plankton in this  
706 subtropical oligotrophic ocean region should be a future research focus. This is also  
707 evidenced in the RAD-B radiolarians, which we found in higher sequence read  
708 abundances in the DCM of eddy CE\_2019\_18N\_20W compared to all other samples.  
709 This entity is also known exclusively from its sequence reads that were retrieved from  
710 a variety of different oceanic regions, globally distributed, from surface waters to the  
711 deep-sea (Sandin 2019). There is unfortunately no detailed knowledge about these  
712 RAD-B radiolarians which prevents us from further exploiting our finding in an  
713 ecological context. However, previous reports suggested that a high abundance of  
714 RAD-B radiolarians may be linked to low-predation pressure (Sandin et al., 2019;  
715 Giner et al., 2020), which, however, still remains to be tested.

716         The collapse of a cyclonic eddy is initiated by a loss of velocity and is initially  
717 characterized by ultra-oligotrophy, followed by leakage and intrusion events (Cesar-  
718 Ribeiro et al., 2020; Liu et al., 2019). Considering these properties, eddy  
719 CE\_2019\_14N\_25W is assumed to be in a late stage of collapse because nutrients  
720 were higher as in the aged eddy CE\_2019\_18N\_20W and plankton communities that  
721 have evolved in the eddy core start to mingle with plankton communities of the  
722 background water. The result is a hybrid protistan community that we obtained from  
723 our samples of eddy CE\_2019\_14N\_25W. In the DCM, this eddy had higher relative  
724 proportions of unassigned Polycystinea compared to the other eddies, emphasizing  
725 our knowledge gaps when it comes to the diversity of these radiolarians with their  
726 opaline silica skeleton in oligotrophic offshore waters. One order within Polycystinea  
727 is Collodaria, of which the DCM of eddy CE\_2019\_14N\_25W had noteworthy higher  
728 relative proportions compared to all other samples. Collodaria are mixotrophs that  
729 flourish in calm and oligotrophic surface waters (Swanberg, 1979). They can prey on  
730 a range of different organisms and size classes, including bacteria, phytoplankton,  
731 ciliates and copepods, and thus, play an important role in the pelagic food web (Biard  
732 et al., 2015). But they also contribute notably to carbon fixation due to their  
733 phototrophic endosymbionts (Michaels et al., 1995), the most common of which is a  
734 dinoflagellate (Probert et al., 2014).

735         In the deeper waters (sub-DCM and OMZ) the protistan communities were  
736 vastly different from the DCM. With increasing depth, the protistan communities of the  
737 youngest eddy CE\_2019\_19N\_18W and the oldest eddy CE\_2019\_14N\_25W  
738 became more similar to the protistan communities in the background waters



739 (references samples). In contrast, the seemingly more robust eddy  
740 CE\_2019\_18N\_20W had distinctively different protistan communities in the deeper  
741 waters compared to the other two eddies and to the reference samples. A  
742 characteristic feature of the background waters was as remarkable increase in the  
743 relative abundance of Haptophyte Clade HAP-4 in the sub-DCM, which was also  
744 mirrored in eddies CE\_2019\_14N\_25W and, to a lesser extent, in eddy  
745 CE\_2019\_19N\_18W. Furthermore, the Haptophyte Clade HAP-5 increased notably in  
746 the sub-DCM in all samples. Both HAP-clades were defined in Egge et al. (2015)  
747 based exclusively on environmental sequences. These authors reported that ASVs of  
748 both clades were previously detected predominantly in deeper, mostly oligotrophic  
749 ocean waters. The ecology of HAP-4 and HAP-5 haptophytes is enigmatic. Our finding  
750 that in the OMZ both haptophyte clades were numerically negligible in all samples,  
751 suggests a sensitivity to oxygen-depletion. Likewise, the composition of radiolarians  
752 changed remarkably from the DCM to the sub-DCM and the OMZ. Changes in  
753 Radiolarian communities with increasing depth are well known, and particular  
754 Spumellarida were preferentially recovered from deeper ocean waters (Not et al.,  
755 2007). The extremely high proportions of Spumellarida in the aged eddy  
756 CE\_2019\_18N\_20W suggests that this taxon group outcompetes other radiolarians  
757 and is a very successful species in the eddy-entrained deep-water masses, including  
758 low-oxygen conditions. Also, in the deeper waters of all samples, Discoba ASVs are  
759 by far dominated by taxonomically unassigned diplomonads. This makes a discussion  
760 about specific differences in the composition of the abundant Discoba sequences and  
761 ASVs impossible. Likewise, we are not capable of linking the higher sequence read  
762 abundances of Dino-Group III in CE\_2019\_19N\_18W to specific properties of this  
763 eddy, because this group consists entirely of environmental sequences from a variety  
764 of different oceanic ecosystems and we have no further information available about  
765 the taxa belonging to this taxonomic unit (Guillou et al., 2008).

766 This emphasizes once more the shortcomings resulting from our extremely  
767 scarce knowledge about protistan diversity and their ecology in the oceans. It is  
768 essential to reveal the identity behind taxonomically unassigned ASVs and to study  
769 the ecology of these organisms if we want to understand ecosystem function(ing) and  
770 processes that lead to selective developments in ecosystems. Interestingly, even  
771 though dinoflagellates also accounted for the numerically most abundant sequence  
772 reads in the sub-DCM and the OMZ, they hardly contributed to the observed changes



773 in beta-diversity patterns across vertical depth profiles within each eddy and the  
774 reference sites. On higher taxonomic levels, the dinoflagellate diversity was  
775 surprisingly uniform across all samples. The best explanation is that the vast majority  
776 of dinoflagellates observed had a parasitoid lifestyle and that they typically infest a  
777 diverse range of hosts such as for example a variety of different radiolarians (Guillou  
778 et al., 2008), which were dominant in all samples. However, we also observed ASVs  
779 taxonomically assigned to free-living dinoflagellates, such as Gymnodiniaceae,  
780 Protoceratiaceae and Heterocapsaceae. These taxon groups, however, did not  
781 notable contribute numerically (in terms of sequence reads) to the obtained  
782 dinoflagellate community and they were also relatively equally contributed across all  
783 samples and depths. This is explained by their high versatility due to their mixotrophic  
784 life style: dinoflagellate can cope with a range of different nutrient regimes and are  
785 among others typical inhabitants of oligotrophic offshore and also coastal waters,  
786 including eddy entrained water masses (Cesar-Ribeiro et al., 2020). Therefore,  
787 dinoflagellates, mixotrophs as well as parasites do not provide a unique signature for  
788 specific eddy conditions such as eddy age, origin or depth.

789

## 790 **Conclusion**

791 Cyclonic eddies that form in the upwelling region of the Northwest African  
792 continental shelf are unique ecosystems with trapped water masses within which  
793 distinctive protistan plankton communities evolve while the eddies age and travel  
794 westwards into sub-tropical oligotrophic offshore waters. A large proportion of the  
795 taxonomic metabarcodes from the protistan plankton communities in the eddies under  
796 surveillance and in the oligotrophic background waters could not be assigned to  
797 ecologically informative taxonomic entities. This demonstrates our knowledge gaps  
798 when it comes to the identification of presumably important members of the protistan  
799 plankton communities in the oceanic region under study. These gaps impede us from  
800 deeper interpretation of our massive sequence data sets to infer further information  
801 about eddies as unique ecosystems. Nevertheless, the data obtained in this study  
802 increased our current knowledge on the effect of mesoscale oceanic features in  
803 offshore waters off Northwest Afrika. Eddies increase the plankton diversity in these  
804 offshore waters to a remarkable extent, thus, providing hotspots in oligotrophic waters  
805 that may play an important role in carbon sequestration and for regional food webs  
806 (including top predators). The three eddies under study harbored distinctively different





807 protistan plankton communities, which is most likely a result of the different  
808 developmental stages of the eddies. But also, seasonal effects as well as the location  
809 of the eddy's formations may play a role for recruiting the initial seed community in the  
810 eddy core and, hence, the further evolution of this community. Unique eddy-specific  
811 communities seem to evolve much faster in the photic zone (DCM) of the eddy cores  
812 compared to deeper layers. This became evident in our observation that even the  
813 youngest eddy CE\_2019\_19N\_18W harbored already a plankton community that was  
814 notably different from the background water community. In the deeper water layers of  
815 the non-photoc zone and the OMZ, it takes a longer time until a unique eddy-specific  
816 ecosystem has established and a characteristic protistan plankton community has  
817 evolved. This became evident in our observation that in deeper water layers of the  
818 youngest eddy the protistan plankton community was relatively similar to the one of  
819 the background waters. The same applied for the oldest eddy, where the deeper water  
820 masses could mingle with background waters, while in the surface waters of this eddy,  
821 plankton communities could still be separated from background waters (even though  
822 there was already a relatively high similarity). This observation seems logic as cyclonic  
823 eddies are typically conical structures that are tapering in the deeper water layers.  
824 Accordingly, the tapering end is the first where intrusions and leakages occur as soon  
825 as the decrease in vorticity heralds in the collapse of an eddy. Thus, we can conclude  
826 that eddy-specific deep-water communities are relatively short lived. Therefore, the  
827 life-span of a mesoscale eddy, which may typically take from few weeks to many  
828 months (Duo et al., 2019) is an especially important criterion for the evolution of  
829 protistan plankton communities in the deep-water layers of an eddy and the way how  
830 eddies influence regional diversity patterns in deeper waters. Only little is known from  
831 previous studies as most investigations focused on eddy surface waters. More  
832 research is needed to better understand the effects of eddies on ecosystem diversity  
833 and function in deeper water layers.

834 Our results showed impressively that the core of mesoscale eddies can support  
835 vastly different ecological key players that have the potential to influence a regional  
836 offshore ecosystem in different ways. Major mechanisms include top-down control  
837 through parasites, carbon fixation through free-living microalgae or phototrophic  
838 endosymbionts, or phagotrophy across different domains of life and organismic size  
839 classes. Concerted efforts are now to reveal whether the numerical dominance of  
840 different taxon groups (in terms of sequence reads) is also mirrored in the functional



841 diversity of the eddy cores, which will reveal further information on the mechanisms

842 how mesoscale ocean features alter sub-tropical oligotrophic offshore ecosystems.

843



## 844 Data availability

845

846 The sequence data files are deposited at the Sequence Read Archive of the National  
847 Center for Biotechnology Information under project number PRJNA795916. All  
848 remaining data will be made available at the PANGEA database.

849

850

## 851 Author contribution

852 SK and TS designed the scientific study, analyzed the data and wrote the paper. MN  
853 and HB contributed in the scientific study design and commented on the paper. TF,  
854 did the eddy reconstruction, sampling site alignment and commented on the paper.

855

## 856 Competing interests

857 The authors declare that they have no conflict of interest.

858

859

## 860 Acknowledgments

861 We thank the captain and the crew of the RV *Meteor* for their support during the M156  
862 and the M160 cruise. We thank the GEOMAR team for the nutrient analyses. This  
863 study is a contribution of the REEBUS project (Role of Eddies in the Carbon Pump of  
864 Eastern Boundary Upwelling Systems) sub-project WP5, funded by the BMBF.

865

866

867

## 868 References

869

870 Abad, D., Albaina, A., Aguirre, M., Laza-Martínez, A., Uriarte, I., Iriarte, A., Villate, F.,  
871 and Estonba, A.: Is metabarcoding suitable for estuarine plankton monitoring? A  
872 comparative study with microscopy, *Mar. Biol.*, 163, 149,  
873 <https://doi.org/10.1007/s00227-016-2920-0>, 2016.

874 Adl, S. M., Bass, D., Lane, C. E., Lukeš, J., Schoch, C. L., Smirnov, A., Agatha, S.,  
875 Berney, C., Brown, M. W., Burki, F., Cárdenas, P., Čepička, I., Chistyakova, L., del  
876 Campo, J., Dunthorn, M., Edvardsen, B., Eglit, Y., Guillou, L., Hampl, V., Heiss, A. A.,  
877 Hoppenrath, M., James, T. Y., Karnkowska, A., Karpov, S., Kim, E., Kolisko, M.,  
878 Kudryavtsev, A., Lahr, D. J. G., Lara, E., Le Gall, L., Lynn, D. H., Mann, D. G.,  
879 Massana, R., Mitchell, E. A. D., Morrow, C., Park, J. S., Pawlowski, J. W., Powell, M.  
880 J., Richter, D. J., Rueckert, S., Shadwick, L., Shimano, S., Spiegel, F. W., Torruella,  
881 G., Youssef, N., Zlatogursky, V., and Zhang, Q.: Revisions to the Classification,  
882 Nomenclature, and Diversity of Eukaryotes, *J. Eukaryot. Microbiol.*, 66, 4–119,  
883 <https://doi.org/10.1111/jeu.12691>, 2019.

884 Alexander, H., Rouco, M., Haley, S. T., Wilson, S. T., Karl, D. M., and Dyhrman, S. T.:  
885 Functional group-specific traits drive phytoplankton dynamics in the oligotrophic  
886 ocean, *Proc. Natl. Acad. Sci.*, 112, E5972–E5979,  
887 <https://doi.org/10.1073/pnas.1518165112>, 2015.



- 888 Anderson, D. M., Hoagland, P., Kaoru, Y., and White, A. W.: Estimated annual  
889 economic impacts from harmful algal blooms (HABs) in the United States, Woods Hole  
890 Oceanographic Institution, Woods Hole, MA, <https://doi.org/10.1575/1912/96>, 2000.
- 891 Barber, R. T.: Picoplankton Do Some Heavy Lifting, *Science*, 315, 777–778,  
892 <https://doi.org/10.1126/science.1137438>, 2007.
- 893 Barlow, R., Lamont, T., Gibberd, M.-J., Airs, R., Jacobs, L., and Britz, K.:  
894 Phytoplankton communities and acclimation in a cyclonic eddy in the southwest Indian  
895 Ocean, *Deep Sea Res. Part Oceanogr. Res. Pap.*, 124, 18–30,  
896 <https://doi.org/10.1016/j.dsr.2017.03.013>, 2017.
- 897 Barton, A. D., Dutkiewicz, S., Flierl, G., Bragg, J., and Follows, M. J.: Patterns of  
898 Diversity in Marine Phytoplankton, *Science*, 327, 1509–1511,  
899 <https://doi.org/10.1126/science.1184961>, 2010.
- 900 Batteen, M. L., Cipriano, N. J., and Monroe, J. T.: A Large-Scale Seasonal Modeling  
901 Study of the California Current System, *J. Oceanogr.*, 59, 545–562,  
902 <https://doi.org/10.1023/B:JOCE.0000009585.24051.cc>, 2003.
- 903 Biard, T., Pillet, L., Decelle, J., Poirier, C., Suzuki, N., and Not, F.: Towards an  
904 Integrative Morpho-molecular Classification of the Collodaria (Polycystinea,  
905 Radiolaria), *Protist*, 166, 374–388, <https://doi.org/10.1016/j.protis.2015.05.002>, 2015.
- 906 Bibby, T. S., Gorbunov, M. Y., Wyman, K. W., and Falkowski, P. G.: Photosynthetic  
907 community responses to upwelling in mesoscale eddies in the subtropical North  
908 Atlantic and Pacific Oceans, *Deep Sea Res. Part II Top. Stud. Oceanogr.*, 55, 1310–  
909 1320, <https://doi.org/10.1016/j.dsr2.2008.01.014>, 2008.
- 910 Brown, S. L., Landry, M. R., Selph, K. E., Jin Yang, E., Rii, Y. M., and Bidigare, R. R.:  
911 Diatoms in the desert: Plankton community response to a mesoscale eddy in the  
912 subtropical North Pacific, *Deep Sea Res. Part II Top. Stud. Oceanogr.*, 55, 1321–  
913 1333, <https://doi.org/10.1016/j.dsr2.2008.02.012>, 2008.
- 914 Burki, F., Sandin, M. M., and Jamy, M.: Diversity and ecology of protists revealed by  
915 metabarcoding, *Curr. Biol.*, 31, R1267–R1280,  
916 <https://doi.org/10.1016/j.cub.2021.07.066>, 2021.
- 917 Cadotte, M. W.: Dispersal and Species Diversity: A Meta-Analysis, *Am. Nat.*, 167,  
918 913–924, <https://doi.org/10.1086/504850>, 2006.
- 919 Callahan, B. J., McMurdie, P. J., Rosen, M. J., Han, A. W., Johnson, A. J. A., and  
920 Holmes, S. P.: DADA2: High-resolution sample inference from Illumina amplicon data,  
921 *Nat. Methods*, 13, 581–583, <https://doi.org/10.1038/nmeth.3869>, 2016.
- 922 Carvalho, A. da C. de O., Mendes, C. R. B., Kerr, R., Azevedo, J. L. L. de, Galdino,  
923 F., and Tavano, V. M.: The impact of mesoscale eddies on the phytoplankton  
924 community in the South Atlantic Ocean: HPLC-CHEMTAX approach, *Mar. Environ.  
925 Res.*, 144, 154–165, <https://doi.org/10.1016/j.marenvres.2018.12.003>, 2019.
- 926 Cesar-Ribeiro, C., Piedras, F. R., da Cunha, L. C., de Lima, D. T., Pinho, L. Q., and  
927 Moser, G. A. O.: Is Oligotrophy an Equalizing Factor Driving Microplankton Species



- 928 Functional Diversity Within Agulhas Rings?, *Front. Mar. Sci.*, 7, 599185,  
929 <https://doi.org/10.3389/fmars.2020.599185>, 2020.
- 930 Chavez, F. P. and Messié, M.: A comparison of Eastern Boundary Upwelling  
931 Ecosystems, *Prog. Oceanogr.*, 83, 80–96,  
932 <https://doi.org/10.1016/j.pocean.2009.07.032>, 2009.
- 933 Chenillat, F., Franks, P. J. S., and Combes, V.: Biogeochemical properties of eddies  
934 in the California Current System, *Geophys. Res. Lett.*, 43, 5812–5820,  
935 <https://doi.org/10.1002/2016GL068945>, 2016.
- 936 Clayton, S., Dutkiewicz, S., Jahn, O., and Follows, M. J.: Dispersal, eddies, and the  
937 diversity of marine phytoplankton: Phytoplankton diversity hotspots, *Limnol.*  
938 *Oceanogr. Fluids Environ.*, 3, 182–197, <https://doi.org/10.1215/21573689-2373515>,  
939 2013.
- 940 Coats, D.W., and Park, M.G.: Parasitism of photosynthetic dinoflagellates by three  
941 strains of *Amoebophrya* (Dinophyta): parasite survival, infectivity, generation time, and  
942 host specificity, *J Phycol*, 38, 520–528, <https://doi.org/10.1046/j.1529-8817.2002.01200.x>, 2002.  
944
- 945 Cullen, J. J.: Subsurface Chlorophyll Maximum Layers: Enduring Enigma or Mystery  
946 Solved?, *Annu. Rev. Mar. Sci.*, 7, 207–239, <https://doi.org/10.1146/annurev-marine-010213-135111>, 2015.  
947
- 948 Dahl, E., Bagøien, E., Edvardsen, B., and Stenseth, N. Chr.: The dynamics of  
949 *Chrysochromulina* species in the Skagerrak in relation to environmental conditions, *J.*  
950 *Sea Res.*, 54, 15–24, <https://doi.org/10.1016/j.seares.2005.02.004>, 2005.
- 951 Decelle, J., Suzuki, N., Mahé, F., de Vargas, C., and Not, F.: Molecular Phylogeny and  
952 Morphological Evolution of the Acantharia (Radiolaria), *Protist*, 163, 435–450,  
953 <https://doi.org/10.1016/j.protis.2011.10.002>, 2012.
- 954 Decelle, J., Martin, P., Paborstava, K., Pond, D. W., Tarling, G., Mahé, F., de Vargas,  
955 C., Lampitt, R., and Not, F.: Diversity, Ecology and Biogeochemistry of Cyst-Forming  
956 Acantharia (Radiolaria) in the Oceans, *PLoS ONE*, 8, e53598,  
957 <https://doi.org/10.1371/journal.pone.0053598>, 2013.
- 958 Degerman, R., Lefébure, R., Byström, P., Båmstedt, U., Larsson, S., and Andersson,  
959 A.: Food web interactions determine energy transfer efficiency and top consumer  
960 responses to inputs of dissolved organic carbon, *Hydrobiologia*, 805, 131–146,  
961 <https://doi.org/10.1007/s10750-017-3298-9>, 2018.
- 962 Dilmahamod, A. F., Karstensen, J., Dietze, H., Löptien, U., and Fennel, K.: Generation  
963 mechanisms of mesoscale eddies in the Mauritanian Upwelling Region, *J. Phys.*  
964 *Oceanogr.*, <https://doi.org/10.1175/JPO-D-21-0092.1>, 2021.
- 965 Duffy, J. E., Cardinale, B. J., France, K. E., McIntyre, P. B., Thébault, E., and Loreau,  
966 M.: The functional role of biodiversity in ecosystems: incorporating trophic complexity,  
967 *Ecol. Lett.*, 10, 522–538, <https://doi.org/10.1111/j.1461-0248.2007.01037.x>, 2007.



- 968 Duo, Z., Wang, W., and Wang, H.: Oceanic Mesoscale Eddy Detection Method Based  
969 on Deep Learning, *Remote Sens.*, 11, 1921, <https://doi.org/10.3390/rs11161921>,  
970 2019.
- 971 Edgar, R. C., Haas, B. J., Clemente, J. C., Quince, C., and Knight, R.: UCHIME  
972 improves sensitivity and speed of chimera detection, *Bioinformatics*, 27, 2194–2200,  
973 <https://doi.org/10.1093/bioinformatics/btr381>, 2011.
- 974 Egge, E. S., Eikrem, W., and Edvardsen, B.: Deep-branching Novel Lineages and  
975 High Diversity of Haptophytes in the Skagerrak (Norway) Uncovered by 454  
976 Pyrosequencing, *J. Eukaryot. Microbiol.*, 62, 121–140,  
977 <https://doi.org/10.1111/jeu.12157>, 2015.
- 978 Eiler, A., Drakare, S., Bertilsson, S., Pernthaler, J., Peura, S., Rofner, C., Simek, K.,  
979 Yang, Y., Znachor, P., and Lindström, E. S.: Unveiling Distribution Patterns of  
980 Freshwater Phytoplankton by a Next Generation Sequencing Based Approach, *PLOS*  
981 *ONE*, 8, e53516, <https://doi.org/10.1371/journal.pone.0053516>, 2013.
- 982 Ewing, B. and Green, P.: Base-calling of automated sequencer traces using phred. II.  
983 Error probabilities, *Genome Res.*, 8, 186–194, 1998.
- 984 Falkowski, P. G.: The role of phytoplankton photosynthesis in global biogeochemical  
985 cycles, *Photosynth. Res.*, 39, 235–258, <https://doi.org/10.1007/BF00014586>, 1994.
- 986 Falkowski, P. G., Barber, R. T., and Smetacek, V.: Biogeochemical Controls and  
987 Feedbacks on Ocean Primary Production, *Science*, 281, 200–206,  
988 <https://doi.org/10.1126/science.281.5374.200>, 1998.
- 989 Fixen, K. R., Starkenburg, S. R., Hovde, B. T., Johnson, S. L., Deodato, C. R.,  
990 Daligault, H. E., Davenport, K. W., Harwood, C. S., and Cattolico, R. A.: Genome  
991 Sequences of Eight Bacterial Species Found in Coculture with the Haptophyte  
992 *Chrysochromulina tobin*, *Genome Announc.*,  
993 <https://doi.org/10.1128/genomeA.01162-16>, 2016.
- 994 Flegontova, O., Flegontov, P., Malviya, S., Audic, S., Wincker, P., de Vargas, C.,  
995 Bowler, C., Lukeš, J., and Horák, A.: Extreme Diversity of Diplonemid Eukaryotes in  
996 the Ocean, *Curr. Biol.*, 26, 3060–3065, <https://doi.org/10.1016/j.cub.2016.09.031>,  
997 2016.
- 998 Flynn, K. J. and Mitra, A.: Building the “perfect beast”: modelling mixotrophic plankton,  
999 *J. Plankton Res.*, 31, 965–992, <https://doi.org/10.1093/plankt/fbp044>, 2009.
- 1000 Forster, D., Lentendu, G., Filker, S., Dubois, E., Wilding, T. A., and Stoeck, T.:  
1001 Improving eDNA-based protist diversity assessments using networks of amplicon  
1002 sequence variants, *Environ. Microbiol.*, 21, 4109–4124, <https://doi.org/10.1111/1462-2920.14764>, 2019.
- 1004 García-Comas, C., Sastri, A. R., Ye, L., Chang, C.-Y., Lin, F.-S., Su, M.-S., Gong, G.-  
1005 C., and Hsieh, C.: Prey size diversity hinders biomass trophic transfer and predator  
1006 size diversity promotes it in planktonic communities, *Proc. R. Soc. B Biol. Sci.*, 283,  
1007 20152129, <https://doi.org/10.1098/rspb.2015.2129>, 2016.



- 1008 Giner, C. R., Pernice, M. C., Balagué, V., Duarte, C. M., Gasol, J. M., Logares, R.,  
1009 and Massana, R.: Marked changes in diversity and relative activity of picoeukaryotes  
1010 with depth in the world ocean, *ISME J.*, 14, 437–449, [https://doi.org/10.1038/s41396-](https://doi.org/10.1038/s41396-019-0506-9)  
1011 019-0506-9, 2020.
- 1012 Grasshoff, K., Kremling, K., and Ehrhardt, M.: *Methods of Seawater Analysis*, John  
1013 Wiley & Sons, 635 pp., 2009.
- 1014 Groisillier, A., Massana, R., Valentin, K., Vaultot, D., and Guillou, L.: Genetic diversity  
1015 and habitats of two enigmatic marine alveolate lineages, *Aquat. Microb. Ecol.*, 42,  
1016 277–291, <https://doi.org/10.3354/ame042277>, 2006.
- 1017 Guillou, L., Viprey, M., Chambouvet, A., Welsh, R. M., Kirkham, A. R., Massana, R.,  
1018 Scanlan, D. J., and Worden, A. Z.: Widespread occurrence and genetic diversity of  
1019 marine parasitoids belonging to *Syndiniales* ( *Alveolata* ), *Environ. Microbiol.*, 10,  
1020 3349–3365, <https://doi.org/10.1111/j.1462-2920.2008.01731.x>, 2008.
- 1021 Guillou, L., Bachar, D., Audic, S., Bass, D., Berney, C., Bittner, L., Boutte, C., Burgaud,  
1022 G., de Vargas, C., Decelle, J., Del Campo, J., Dolan, J. R., Dunthorn, M., Edvardsen,  
1023 B., Holzmann, M., Kooistra, W. H. C. F., Lara, E., Le Bescot, N., Logares, R., Mahé,  
1024 F., Massana, R., Montresor, M., Morard, R., Not, F., Pawlowski, J., Probert, I.,  
1025 Sauvadet, A.-L., Siano, R., Stoeck, T., Vaultot, D., Zimmermann, P., and Christen, R.:  
1026 The Protist Ribosomal Reference database (PR2): a catalog of unicellular eukaryote  
1027 small sub-unit rRNA sequences with curated taxonomy, *Nucleic Acids Res.*, 41, D597-  
1028 604, <https://doi.org/10.1093/nar/gks1160>, 2013.
- 1029 Hall, C. and Lutjeharms, J. R. E.: Cyclonic eddies identified in the Cape Basin of the  
1030 South Atlantic Ocean, *J. Mar. Syst.*, 85, 1–10,  
1031 <https://doi.org/10.1016/j.jmarsys.2010.10.003>, 2011.
- 1032 Hallegraef, G. M., Anderson, D. M., Belin, C., Bottein, M.-Y. D., Bresnan, E., Chinain,  
1033 M., Enevoldsen, H., Iwataki, M., Karlson, B., McKenzie, C. H., Sunesen, I., Pitcher, G.  
1034 C., Provoost, P., Richardson, A., Schweibold, L., Tester, P. A., Trainer, V. L., Yñiguez,  
1035 A. T., and Zingone, A.: Perceived global increase in algal blooms is attributable to  
1036 intensified monitoring and emerging bloom impacts, *Commun. Earth Environ.*, 2, 117,  
1037 <https://doi.org/10.1038/s43247-021-00178-8>, 2021.
- 1038 Hernández-Hernández, N., Arístegui, J., Montero, M. F., Velasco-Senovilla, E., Baltar,  
1039 F., Marrero-Díaz, Á., Martínez-Marrero, A., and Rodríguez-Santana, Á.: Drivers of  
1040 Plankton Distribution Across Mesoscale Eddies at Submesoscale Range, *Front. Mar.  
1041 Sci.*, 7, 667, <https://doi.org/10.3389/fmars.2020.00667>, 2020.
- 1042 Higgins, H. W., Wright, S. W., and Schluter, L.: Quantitative interpretation of  
1043 chemotaxonomic pigment data, 2011.
- 1044 Hovde, B. T., Deodato, C. R., Hunsperger, H. M., Ryken, S. A., Yost, W., Jha, R. K.,  
1045 Patterson, J., Jr, R. J. M., Barlow, S. B., Starkenburg, S. R., and Cattolico, R. A.:  
1046 Genome Sequence and Transcriptome Analyses of *Chrysochromulina tobin*:  
1047 Metabolic Tools for Enhanced Algal Fitness in the Prominent Order Prymnesiales  
1048 (Haptophyceae), *PLOS Genet.*, 11, e1005469,  
1049 <https://doi.org/10.1371/journal.pgen.1005469>, 2015.



- 1050 Ibarbalz, F. M., Henry, N., Brandão, M. C., Martini, S., Busseni, G., Byrne, H., Coelho,  
1051 L. P., Endo, H., Gasol, J. M., Gregory, A. C., Mahé, F., Rigonato, J., Royo-Llonch, M.,  
1052 Salazar, G., Sanz-Sáez, I., Scalco, E., Soviadan, D., Zayed, A. A., Zingone, A.,  
1053 Labadie, K., Ferland, J., Marec, C., Kandels, S., Picheral, M., Dimier, C., Poulain, J.,  
1054 Pisarev, S., Carmichael, M., Pesant, S., Babin, M., Boss, E., Iudicone, D., Jaillon, O.,  
1055 Acinas, S. G., Ogata, H., Pelletier, E., Stemmann, L., Sullivan, M. B., Sunagawa, S.,  
1056 Bopp, L., de Vargas, C., Karp-Boss, L., Wincker, P., Lombard, F., Bowler, C., Zinger,  
1057 L., Acinas, S. G., Babin, M., Bork, P., Boss, E., Bowler, C., Cochrane, G., de Vargas,  
1058 C., Follows, M., Gorsky, G., Grimsley, N., Guidi, L., Hingamp, P., Iudicone, D., Jaillon,  
1059 O., Kandels, S., Karp-Boss, L., Karsenti, E., Not, F., Ogata, H., Pesant, S., Poulton,  
1060 N., Raes, J., Sardet, C., Speich, S., Stemmann, L., Sullivan, M. B., Sunagawa, S., and  
1061 Wincker, P.: Global Trends in Marine Plankton Diversity across Kingdoms of Life, *Cell*,  
1062 179, 1084–1097.e21, <https://doi.org/10.1016/j.cell.2019.10.008>, 2019.
- 1063 Johansson, N. and Granéli, E.: Cell density, chemical composition and toxicity of  
1064 *Chrysochromulina polylepis* (Haptophyta) in relation to different N:P supply ratios,  
1065 *Mar. Biol.*, 135, 209–217, <https://doi.org/10.1007/s002270050618>, 1999.
- 1066 Klintzsch, T., Langer, G., Nehrke, G., Wieland, A., Lenhart, K., and Keppler, F.:  
1067 Methane production by three widespread marine phytoplankton species: release  
1068 rates, precursor compounds, and potential relevance for the environment,  
1069 *Biogeosciences*, 16, 4129–4144, <https://doi.org/10.5194/bg-16-4129-2019>, 2019.
- 1070 Kurian, J., Colas, F., Capet, X., McWilliams, J. C., and Chelton, D. B.: Eddy properties  
1071 in the California Current System, *J. Geophys. Res. Oceans*, 116,  
1072 <https://doi.org/10.1029/2010JC006895>, 2011.
- 1073 Lamont, T. and Barlow, R.: Contrasting hydrography and phytoplankton distribution in  
1074 the upper layers of cyclonic eddies in the Mozambique Basin and Mozambique  
1075 Channel, *Afr. J. Mar. Sci.*, 39, 293–306,  
1076 <https://doi.org/10.2989/1814232X.2017.1367722>, 2017.
- 1077 Lane, D. J.: 16S/23S rRNA sequencing, in: *Nucleic Acid Techniques in Bacterial*  
1078 *Systematics*, edited by: Stackebrandt, E. and Goodfellow, M., John Wiley and Sons,  
1079 Chichester, UK, 1991.
- 1080 Lara, E., Moreira, D., Vereshchaka, A., and López-García, P.: Pan-oceanic distribution  
1081 of new highly diverse clades of deep-sea diplomonads, *Environ. Microbiol.*, 11, 47–55,  
1082 <https://doi.org/10.1111/j.1462-2920.2008.01737.x>, 2009.
- 1083 Leach, H. and Strass, V.: Cyclonic eddies and upper thermocline fine-scale structures  
1084 in the Antarctic Circumpolar Current, *Ocean Dyn.*, 69, 157–173,  
1085 <https://doi.org/10.1007/s10236-018-1241-x>, 2019.
- 1086 Legendre, L. and Michaud, J.: Flux of biogenic carbon in oceans: size-dependent  
1087 regulation by pelagic food webs, *Mar. Ecol. Prog. Ser.*, 164, 1–11,  
1088 <https://doi.org/10.3354/meps164001>, 1998.
- 1089 Liss, P. S., Malin, G., Turner, S. M., and Holligan, P. M.: Dimethyl sulphide and  
1090 *Phaeocystis*: A review, *J. Mar. Syst.*, 5, 41–53, [https://doi.org/10.1016/0924-7963\(94\)90015-9](https://doi.org/10.1016/0924-7963(94)90015-9), 1994.





- 1092 Liu, T., Abernathey, R., Sinha, A., and Chen, D.: Quantifying Eulerian Eddy Leakiness  
1093 in an Idealized Model, *J. Geophys. Res. Oceans*, 124, 8869–8886,  
1094 <https://doi.org/10.1029/2019JC015576>, 2019.
- 1095 López-García, P., Rodríguez-Valera, F., Pedrós-Alió, C., and Moreira, D.: Unexpected  
1096 diversity of small eukaryotes in deep-sea Antarctic plankton, *Nature*, 409, 603–607,  
1097 <https://doi.org/10.1038/35054537>, 2001.
- 1098 Mars Brisbin, M., Mesrop, L. Y., Grossmann, M. M., and Mitarai, S.: Intra-host  
1099 Symbiont Diversity and Extended Symbiont Maintenance in Photosymbiotic  
1100 Acantharea (Clade F), *Front. Microbiol.*, 9, 1998,  
1101 <https://doi.org/10.3389/fmicb.2018.01998>, 2018.
- 1102 Mars Brisbin, M., Brunner, O. D., Grossmann, M. M., and Mitarai, S.: Paired high-  
1103 throughput, in situ imaging and high-throughput sequencing illuminate acantharian  
1104 abundance and vertical distribution, *Limnol. Oceanogr.*, 65, 2953–2965,  
1105 <https://doi.org/10.1002/lno.11567>, 2020.
- 1106 Martin, C. L. and Tortell, P. D.: Bicarbonate transport and extracellular carbonic  
1107 anhydrase in marine diatoms, *Physiol. Plant.*, 133, 106–116,  
1108 <https://doi.org/10.1111/j.1399-3054.2008.01054.x>, 2008.
- 1109 Martin, P., Allen, J. T., Cooper, M. J., Johns, D. G., Lampitt, R. S., Sanders, R., and  
1110 Teagle, D. A. H.: Sedimentation of acantharian cysts in the Iceland Basin: Strontium  
1111 as a ballast for deep ocean particle flux, and implications for acantharian reproductive  
1112 strategies, *Limnol. Oceanogr.*, 55, 604–614,  
1113 <https://doi.org/10.4319/lno.2010.55.2.0604>, 2010.
- 1114 McGillicuddy, D. J.: Mechanisms of Physical-Biological-Biogeochemical Interaction at  
1115 the Oceanic Mesoscale, *Annu. Rev. Mar. Sci.*, 8, 125–159,  
1116 <https://doi.org/10.1146/annurev-marine-010814-015606>, 2016.
- 1117 Medlin, L., Elwood, H. J., Stickel, S., and Sogin, M. L.: The characterization of  
1118 enzymatically amplified eukaryotic 16S-like rRNA-coding regions, *Gene*, 71, 491–499,  
1119 [https://doi.org/10.1016/0378-1119\(88\)90066-2](https://doi.org/10.1016/0378-1119(88)90066-2), 1988.
- 1120 Michaels, A. F. and Silver, M. W.: Primary production, sinking fluxes and the microbial  
1121 food web, *Deep Sea Res. Part Oceanogr. Res. Pap.*, 35, 473–490,  
1122 [https://doi.org/10.1016/0198-0149\(88\)90126-4](https://doi.org/10.1016/0198-0149(88)90126-4), 1988.
- 1123 Michaels, A. F., Caron, D. A., Swanberg, N. R., Howse, F. A., and Michaels, C. M.:  
1124 Planktonic sarcodines (Acantharia, Radiolaria, Foraminifera) in surface waters near  
1125 Bermuda: abundance, biomass and vertical flux, *J. Plankton Res.*, 17, 131–163,  
1126 <https://doi.org/10.1093/plankt/17.1.131>, 1995.
- 1127 Not, F., Gausling, R., Azam, F., Heidelberg, J. F., and Worden, A. Z.: Vertical  
1128 distribution of picoeukaryotic diversity in the Sargasso Sea, *Environ. Microbiol.*, 9,  
1129 1233–1252, <https://doi.org/10.1111/j.1462-2920.2007.01247.x>, 2007.



- 1130 Oksanen, J., Blanchet, F.G., Friendly, M., Kindt, R., Legendre, P., McGlinn, D.,  
1131 Minchin, P.R., O'Hara, R.B., Simpson, G.L., Solymos, P., Stevens, M.H.H., Szoecs,  
1132 E., Wagner, H.: vegan: Community ecology package. R package version 2.5-7, 2020.  
1133
- 1134 d'Ovidio, F., De Monte, S., Alvain, S., Dandonneau, Y., and Levy, M.: Fluid dynamical  
1135 niches of phytoplankton types, *Proc. Natl. Acad. Sci.*, 107, 18366–18370,  
1136 <https://doi.org/10.1073/pnas.1004620107>, 2010.
- 1137 Owen, R. W.: Eddies of the California Current System: Physical and Ecological  
1138 Characteristics, 1980.
- 1139 Pelegrí, J. L., Arístegui, J., Cana, L., González-Dávila, M., Hernández-Guerra, A.,  
1140 Hernández-León, S., Marrero-Díaz, A., Montero, M. F., Sangrà, P., and Santana-  
1141 Casiano, M.: Coupling between the open ocean and the coastal upwelling region off  
1142 northwest Africa: water recirculation and offshore pumping of organic matter, *J. Mar.  
1143 Syst.*, 54, 3–37, <https://doi.org/10.1016/j.jmarsys.2004.07.003>, 2005.
- 1144 Probert, I., Siano, R., Poirier, C., Decelle, J., Biard, T., Tuji, A., Suzuki, N., and Not,  
1145 F.: *B. randtodinium* gen. nov. and *B. nutricula* comb. Nov. (Dinophyceae), a  
1146 dinoflagellate commonly found in symbiosis with polycystine radiolarians, *J. Phycol.*,  
1147 50, 388–399, <https://doi.org/10.1111/jpy.12174>, 2014.
- 1148 Ramond, P., Siano, R., Schmitt, S., de Vargas, C., Marié, L., Memery, L., and  
1149 Sourisseau, M.: Phytoplankton taxonomic and functional diversity patterns across a  
1150 coastal tidal front, *Sci. Rep.*, 11, 2682, <https://doi.org/10.1038/s41598-021-82071-0>,  
1151 2021.
- 1152 Rocke, E., Cheung, S., Gebe, Z., Dames, N. R., Liu, H., and Moloney, C. L.: Marine  
1153 Microbial Community Composition During the Upwelling Season in the Southern  
1154 Benguela, *Front. Mar. Sci.*, 7, 255, <https://doi.org/10.3389/fmars.2020.00255>, 2020.
- 1155 San Martin, E., Irigoien, X., Roger P, H., Urrutia, Â. L.-, Zubkov, M. V., and Heywood,  
1156 J. L.: Variation in the transfer of energy in marine plankton along a productivity gradient  
1157 in the Atlantic Ocean, *Limnol. Oceanogr.*, 51, 2084–2091,  
1158 <https://doi.org/10.4319/lo.2006.51.5.2084>, 2006.
- 1159 Sandín, M. M.: Diversity and Evolution of Nassellaria and Spumellaria (Radiolaria).  
1160 Diss. Sorbonne Université, 2019.
- 1161 Scheckenbach, F., Hausmann, K., Wylezich, C., Weitere, M., and Arndt, H.: Large-  
1162 scale patterns in biodiversity of microbial eukaryotes from the abyssal sea floor, *Proc.  
1163 Natl. Acad. Sci.*, 107, 115–120, <https://doi.org/10.1073/pnas.0908816106>, 2010.
- 1164 Schoemann, V., Becquevort, S., Stefels, J., Rousseau, V., and Lancelot, C.:  
1165 Phaeocystis blooms in the global ocean and their controlling mechanisms: a review,  
1166 *J. Sea Res.*, 53, 43–66, <https://doi.org/10.1016/j.seares.2004.01.008>, 2005.
- 1167 Shannon, C. E., and Weaver, W.: The Mathematical Theory of Communication, Univ.  
1168 of Ill. Press, Urbana, Ill, 1949.  
1169



- 1170 Sherr, E. B. and Sherr, B. F.: Bacterivory and herbivory: Key roles of phagotrophic  
1171 protists in pelagic food webs, *Microb. Ecol.*, 28, 223–235,  
1172 <https://doi.org/10.1007/BF00166812>, 1994.
- 1173 Siano, R., Alves-de-Souza, C., Foulon, E., Bendif, E. M., Simon, N., Guillou, L., and  
1174 Not, F.: Distribution and host diversity of Amoebozoa parasites across  
1175 oligotrophic waters of the Mediterranean Sea, *Biogeosciences*, 8, 267–278,  
1176 <https://doi.org/10.5194/bg-8-267-2011>, 2011.
- 1177 Singer, D., Seppey, C. V. W., Lentendu, G., Dunthorn, M., Bass, D., Belbahri, L.,  
1178 Blandenier, Q., Debroas, D., de Groot, G. A., de Vargas, C., Domaizon, I., Duckert,  
1179 C., Izaguirre, I., Koenig, I., Mataloni, G., Schiaffino, M. R., Mitchell, E. A. D., Geisen,  
1180 S., and Lara, E.: Protist taxonomic and functional diversity in soil, freshwater and  
1181 marine ecosystems, *Environ. Int.*, 146, 106262,  
1182 <https://doi.org/10.1016/j.envint.2020.106262>, 2021.
- 1183 Smith, W. O., Codispoti, L. A., Nelson, D. M., Manley, T., Buskey, E. J., Niebauer, H.  
1184 J., and Cota, G. F.: Importance of Phaeocystis blooms in the high-latitude ocean  
1185 carbon cycle, *Nature*, 352, 514–516, <https://doi.org/10.1038/352514a0>, 1991.
- 1186 Spellerberg, I. F. and Fedor, P. J.: A tribute BlackwellScience,Ltd to Claude Shannon  
1187 (1916 –2001) and a plea for more rigorous use of species richness, species diversity  
1188 and the ‘Shannon–Wiener’ Index, 3, <https://doi.org/10.1046/j.1466-822X.2003.00015.x>, 2003.  
1189  
1190
- 1191 Stoeck, T., Bass, D., Nebel, M., Christen, R., Jones, M. D. M., Breiner, H.-W., and  
1192 Richards, T. A.: Multiple marker parallel tag environmental DNA sequencing reveals a  
1193 highly complex eukaryotic community in marine anoxic water, *Mol. Ecol.*, 19, 21–31,  
1194 <https://doi.org/10.1111/j.1365-294X.2009.04480.x>, 2010.
- 1195 Strickland, J.D.H. and Parsons, T.R.: A Practical Handbook of Seawater Analysis, J.  
1196 Fish. Res. Board Can, 167, 1-311, 1968.  
1197
- 1198 Swanberg, N. R.: The ecology of colonial radiolarians: their colony morphology,  
1199 trophic interactions and associations, behavior, distribution, and the photosynthesis of  
1200 their symbionts, Massachusetts Institute of Technology and Woods Hole  
1201 Oceanographic Institution, 1979.
- 1202 Tragin, M. and Vaultot, D.: Green microalgae in marine coastal waters: The Ocean  
1203 Sampling Day (OSD) dataset, *Sci. Rep.*, 8, 14020, <https://doi.org/10.1038/s41598-018-32338-w>, 2018.  
1204
- 1205 Van Oostende, N., Dussin, R., Stock, C. A., Barton, A. D., Curchitser, E., Dunne, J.  
1206 P., and Ward, B. B.: Simulating the ocean’s chlorophyll dynamic range from coastal  
1207 upwelling to oligotrophy, *Prog. Oceanogr.*, 168, 232–247,  
1208 <https://doi.org/10.1016/j.pocean.2018.10.009>, 2018.
- 1209 Vargas, C. A., Martínez, R. A., Cuevas, L. A., Pavez, M. A., Cartes, C., González, H.  
1210 E., Escribano, R., and Daneri, G.: The relative importance of microbial and classical  
1211 food webs in a highly productive coastal upwelling area, *Limnol. Oceanogr.*, 52, 1495–  
1212 1510, <https://doi.org/10.4319/lo.2007.52.4.1495>, 2007.



- 1213 Vargas, C. de, Audic, S., Henry, N., Decelle, J., Mahé, F., Logares, R., Lara, E.,  
1214 Berney, C., Bescot, N. L., Probert, I., Carmichael, M., Poulain, J., Romac, S., Colin,  
1215 S., Aury, J.-M., Bittner, L., Chaffron, S., Dunthorn, M., Engelen, S., Flegontova, O.,  
1216 Guidi, L., Horák, A., Jaillon, O., Lima-Mendez, G., Lukeš, J., Malviya, S., Morard, R.,  
1217 Mulot, M., Scalco, E., Siano, R., Vincent, F., Zingone, A., Dimier, C., Picheral, M.,  
1218 Searson, S., Kandels-Lewis, S., Coordinators, T. O., Acinas, S. G., Bork, P., Bowler,  
1219 C., Gorsky, G., Grimsley, N., Hingamp, P., Iudicone, D., Not, F., Ogata, H., Pesant,  
1220 S., Raes, J., Sieracki, M. E., Speich, S., Stemmann, L., Sunagawa, S., Weissenbach,  
1221 J., Wincker, P., Karsenti, E., Boss, E., Follows, M., Karp-Boss, L., Krzic, U., Reynaud,  
1222 E. G., Sardet, C., Sullivan, M. B., and Velayoudon, D.: Eukaryotic plankton diversity in  
1223 the sunlit ocean, *Science*, <https://doi.org/10.1126/science.1261605>, 2015.
- 1224 Visco, J. A., Apothéoz-Perret-Gentil, L., Cordonier, A., Esling, P., Pillet, L., and  
1225 Pawlowski, J.: Environmental Monitoring: Inferring the Diatom Index from Next-  
1226 Generation Sequencing Data, *Environ. Sci. Technol.*, 49, 7597–7605,  
1227 <https://doi.org/10.1021/es506158m>, 2015.
- 1228 Ward, B. A., Dutkiewicz, S., Jahn, O., and Follows, M. J.: A size-structured food-web  
1229 model for the global ocean, *Limnol. Oceanogr.*, 57, 1877–1891,  
1230 <https://doi.org/10.4319/lo.2012.57.6.1877>, 2012.
- 1231 Ward, B. A., Cael, B. B., Collins, S., and Young, C. R.: Selective constraints on global  
1232 plankton dispersal, *Proc. Natl. Acad. Sci.*, 118, e2007388118,  
1233 <https://doi.org/10.1073/pnas.2007388118>, 2021.
- 1234 Wickham, H., Chang, W., and Wickham, M. H.: Package ‘ggplot2’. Create elegant data  
1235 visualisations using the grammar of graphics. Version, 2(1), 1-189, 2016.  
1236
- 1237 Wilhelm, W. L.: Die Bestimmung des im Wasser gelösten Sauerstoffes, *Ber. Dtsch.*  
1238 *Chem. Ges.*, 21, 2843-2854, 1888.  
1239
- 1240 Wilken, S., Choi, C. J., and Worden, A. Z.: Contrasting Mixotrophic Lifestyles Reveal  
1241 Different Ecological Niches in Two Closely Related Marine Protists, *J. Phycol.*, 56, 52–  
1242 67, <https://doi.org/10.1111/jpy.12920>, 2020.
- 1243 Wu, C.-R. and Chiang, T.-L.: Mesoscale eddies in the northern South China Sea,  
1244 *Deep Sea Res. Part II Top. Stud. Oceanogr.*, 54, 1575–1588,  
1245 <https://doi.org/10.1016/j.dsr2.2007.05.008>, 2007.
- 1246  
1247  
1248  
1249  
1250  
1251  
1252



1253 **Figure legends**

1254

1255 **Figure 1.** Schematic representation of eddy locations at the time of sampling, of  
1256 individual sample locations within each eddy (CE\_2019\_19N\_18W,  
1257 CE\_2019\_18N\_20W, CE\_2019\_14N\_25W) and at the two background waters  
1258 (reference sites CVOO and CB).

1259

1260 **Figure 2.** PCA of eddy stations and background waters (reference sites CVOO and  
1261 CB) based on physico-chemical parameters

1262

1263 **Figure 3.** ASV richness and Shannon Index  $H'$  as measures of alpha-diversity of  
1264 protistan plankton communities in the DCM (a), sub-DCM (b) and OMZ (c) of the three  
1265 eddies under study (CE\_2019\_19N\_18W, CE\_2019\_18N\_20W,  
1266 CE\_2019\_14N\_25W) and the background reference waters (CVOO and CB).

1267

1268 **Figure 4.** Effect of the three eddies under study (CE\_2019\_19N\_18W,  
1269 CE\_2019\_18N\_20W, CE\_2019\_14N\_25W) on regional ASV richness and Shannon  
1270 Index  $H'$  of protistan plankton communities in the DCM (a), sub-DCM (b) and OMZ (c).  
1271 The y-axis shows a decrease of richness and diversity in the two background waters  
1272 CVOO and CB resulting from the eddy-specific communities that were transported into  
1273 the offshore background waters during the westward-bound eddy trajectories.

1274

1275 **Figure 5.** Beta-diversity (NMDS based on BC-distances of ASV-to-sample matrix) of  
1276 protistan plankton communities in the DCM (red), sub-DCM (green) and OMZ (blue)  
1277 of the three eddies under study (CE\_2019\_19N\_18W, CE\_2019\_18N\_20W,  
1278 CE\_2019\_14N\_25W, coded by symbol shape). NMDS stress = 0.121. Correlation  
1279 results of environmental parameters with NMDS axes are shown in Table 2.

1280

1281 **Figure 6.** Partitioning of diversity (Bray Curtis distance-based dendrograms) of  
1282 protistan plankton communities in the three eddies under study and the two  
1283 background waters (reference sites CVOO and CB) for the DCM (a), the sub-DCM (b)  
1284 and the OMZ (c).

1285

1286



1287 **Tables**

1288 **Table 1.** Coordinates of sample sites located inside the mesoscale eddy structures

1289 and the two reference sites with the corresponding sampling dates and ship cruises.

Sampling station	latitude	longitude	Reference/Eddy	date	cruise
Reference_CB	21.17	-20.92	Reference	07.12.2019	M156
CE_2019_19N_18W	18.58	-18.08	Eddy	07.22.2019	M156
Reference_CVOO	17.59	-24.28	Reference	12.09.2019	M160
CE_2019_14N_25W(1)	14.44	-25.25	Eddy	12.13.2019	M160
CE_2019_14N_25W(2)	14.62	-25.07	Eddy	12.13.2019	M160
CE_2019_14N_25W(3)	14.72	-25.49	Eddy	12.15.2019	M160
CE_2019_18N_20W(1)	17.61	-20.60	Eddy	11.30.2019	M160
CE_2019_18N_20W(2)	17.81	-20.80	Eddy	12.02.2019	M160
CE_2019_18N_20W(3)	17.82	-20.60	Eddy	12.03.2019	M160
CE_2019_18N_20W(4)	17.81	-20.41	Eddy	12.03.2019	M160

1290

1291



1292 **Table 2.** Correlation results from *envfit* analyses of environmental parameters and  
1293 NMDS axes 1 and 2 of NMDS analyses (beta diversity) of protistan plankton  
1294 communities in the DCM, sub-DCM and OMZ of the three eddies under study (see  
1295 Fig. 4).

Parameter	NMDS1 axis	NMDS2 axis	R <sup>2</sup>	p-value
Nitrate	0,85	-0,41	0,90	1,00E-04
Phosphate	0,84	-0,43	0,88	1,00E-04
Orthosilicic acid	0,85	-0,40	0,87	1,00E-04
Temperature	-0,84	0,48	0,93	1,00E-04
Salinity	-0,76	0,45	0,77	1,00E-04
Diss. Oxygen	-0,66	0,49	0,68	1,00E-04
Density	0,81	-0,47	0,88	1,00E-04
Fluorescence	-0,86	0,33	0,84	1,00E-04
Turbidity	-0,78	-0,12	0,62	2,00E-04

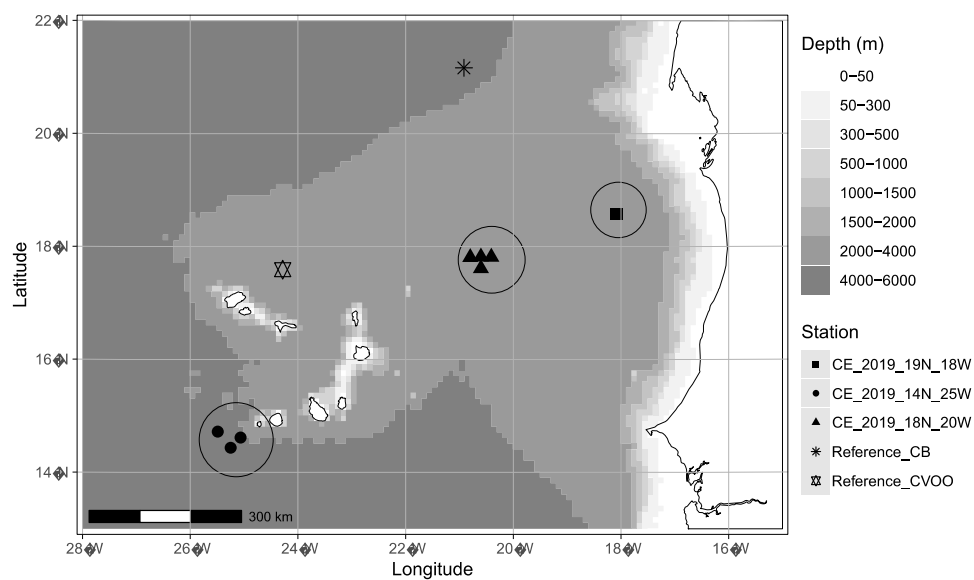
1296

1297



1298 **Figures**

Figure 1



1299

1300

1301

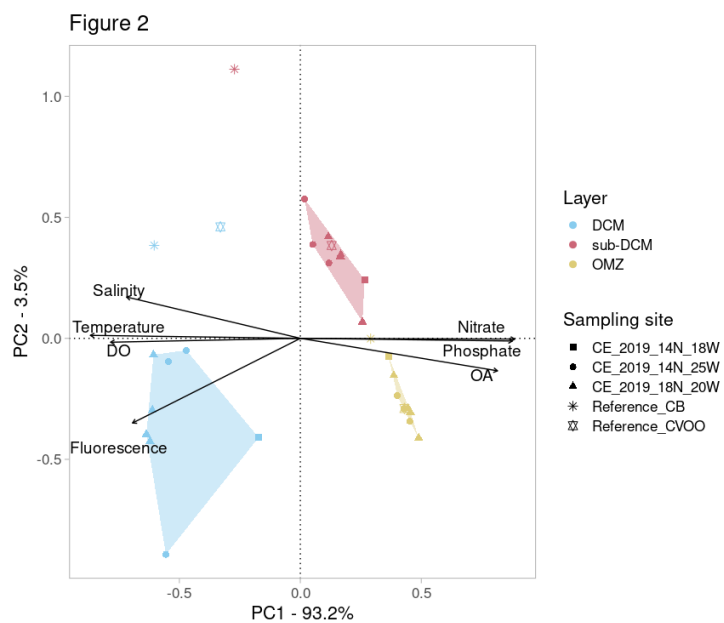
1302





1303

1304



1305

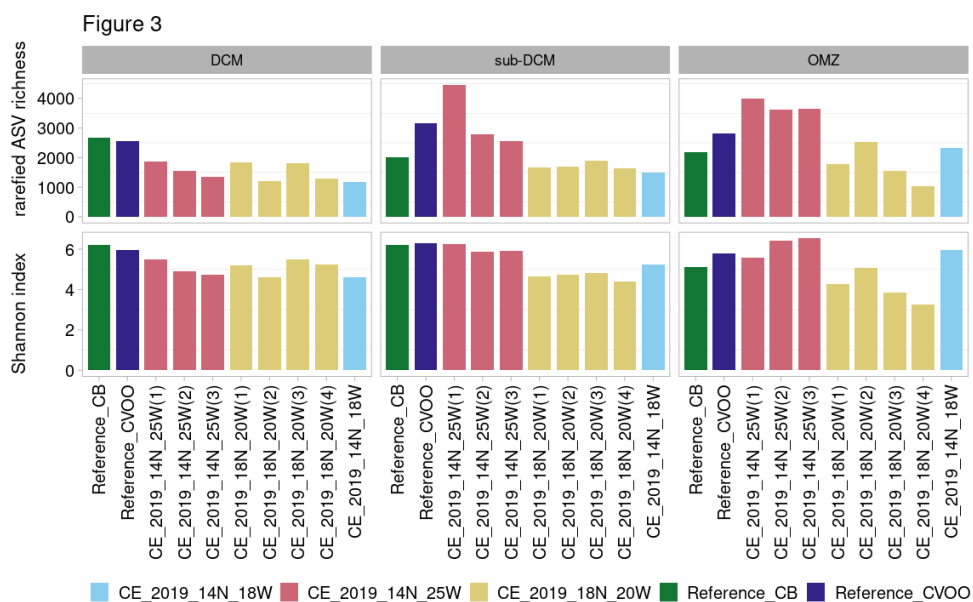
1306

1307



1308

1309



1310

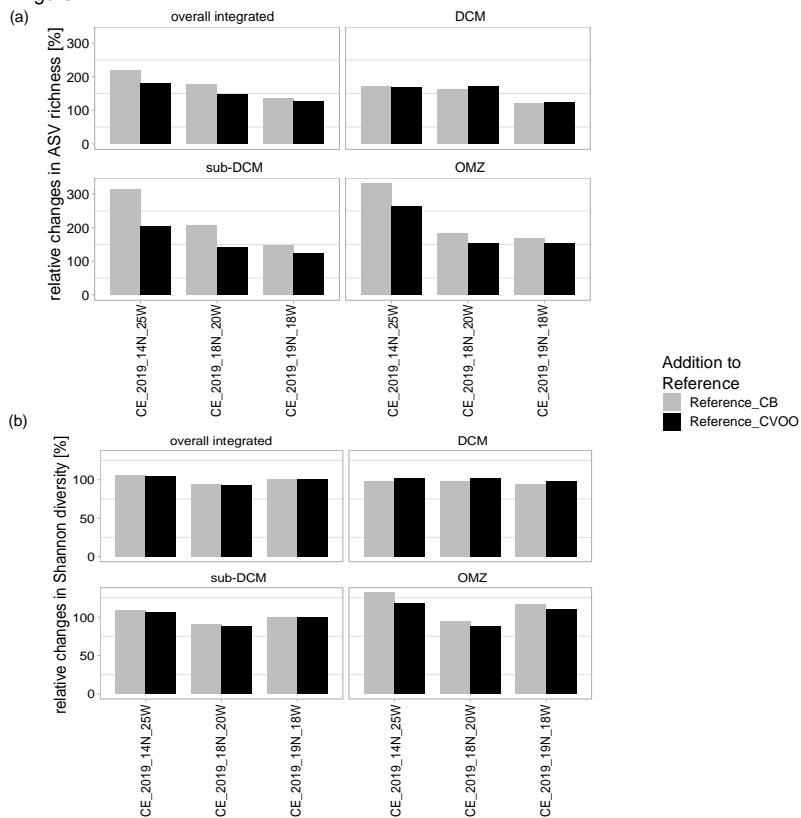
1311

1312

1313



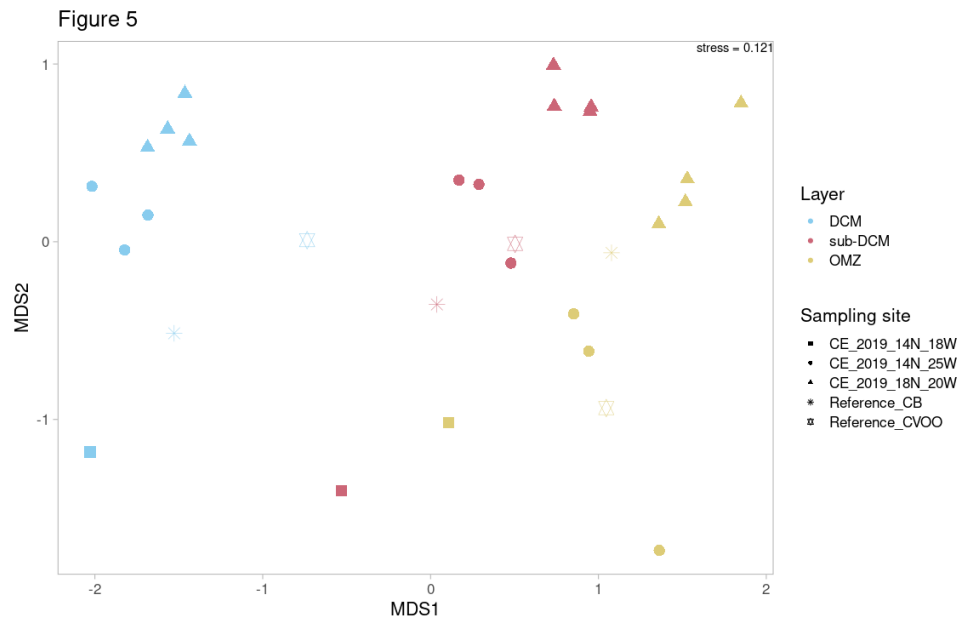
Figure 4



1314  
1315  
1316



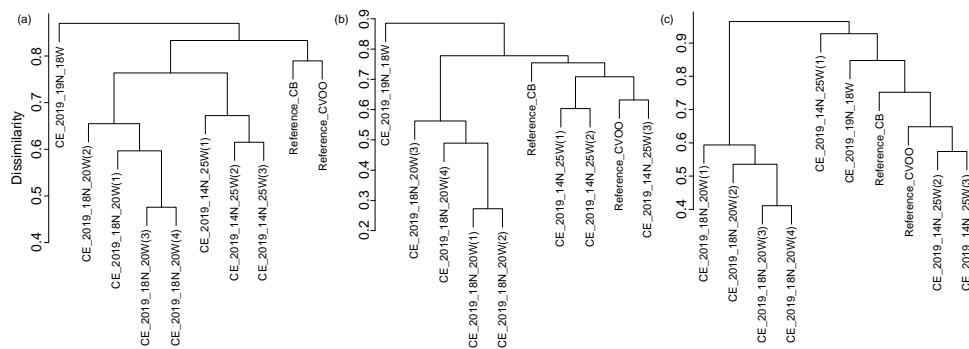
1317  
1318



1319  
1320  
1321  
1322  
1323



Figure 6



1324  
1325